

AD-A152 703

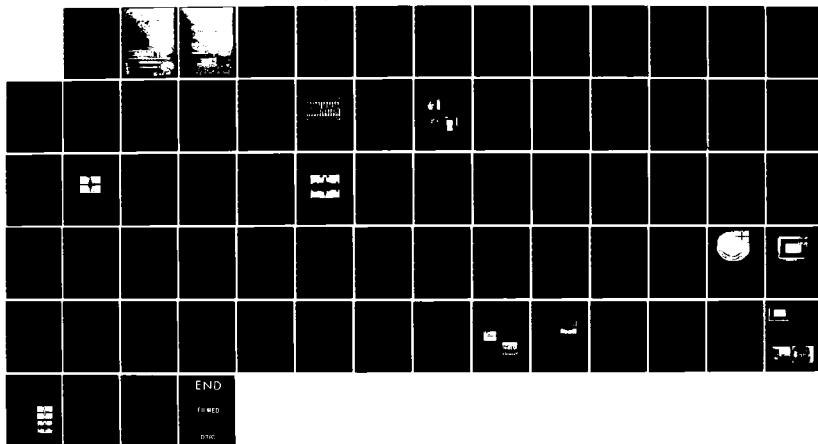
RESEARCH ON SUPERCONDUCTIVE SIGNAL-PROCESSING DEVICES
(U) MASSACHUSETTS INST OF TECH LEXINGTON LINCOLN LAB
R W RALSTON 30 NOV 84 ESD-TR-84-293 F19628-85-C-0002

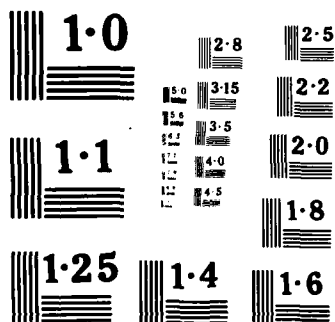
1/1

UNCLASSIFIED

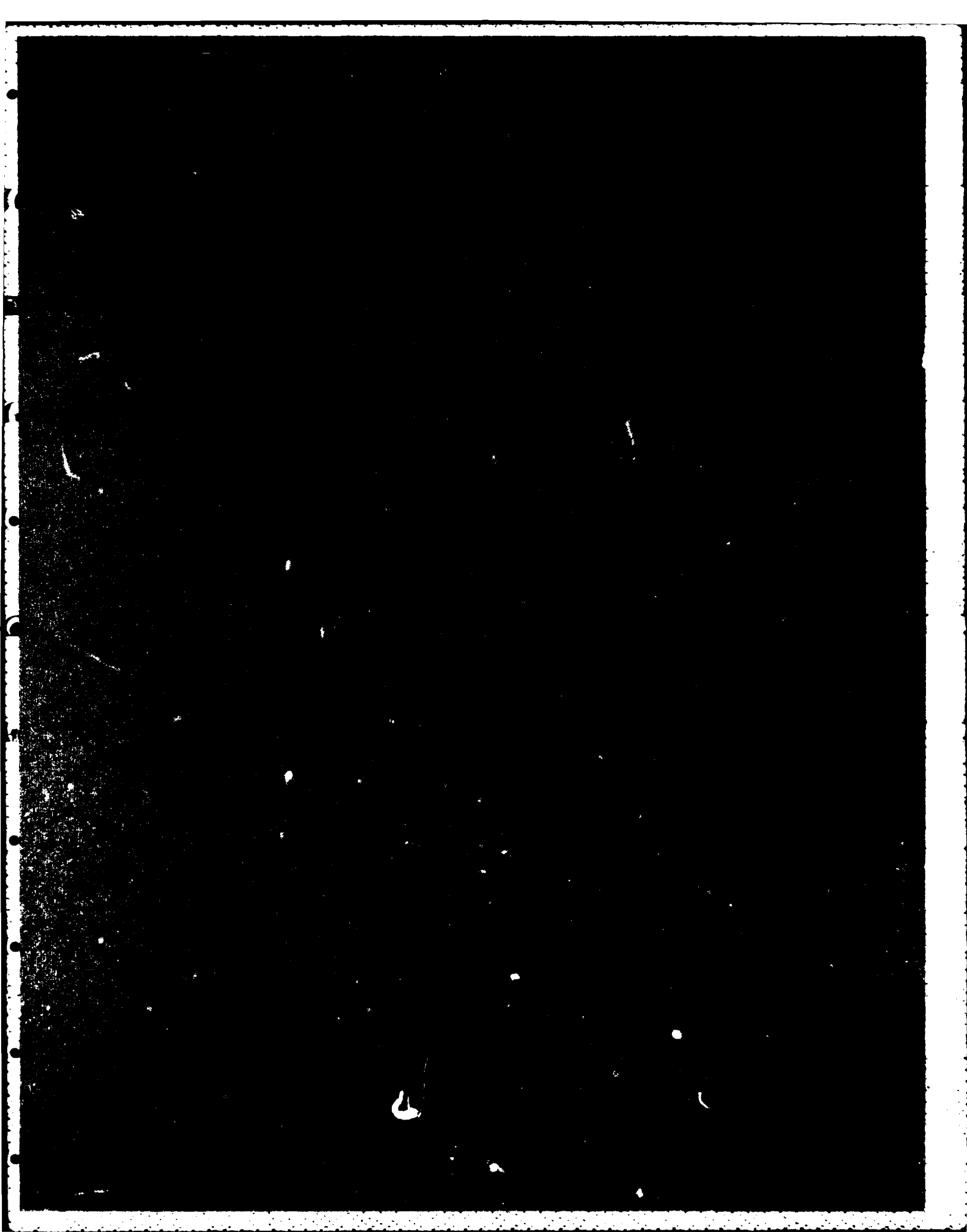
F/G 9/5

NL





AD-A152 703



**MASSACHUSETTS INSTITUTE OF TECHNOLOGY
LINCOLN LABORATORY**

**RESEARCH ON SUPERCONDUCTIVE
SIGNAL-PROCESSING DEVICES**

**ANNUAL REPORT
TO THE
AIR FORCE OFFICE OF SCIENTIFIC RESEARCH
ELECTRONICS AND SOLID STATE SCIENCES DIVISION**

R.W. RALSTON

Group 86

1 OCTOBER 1983 30 SEPTEMBER 1984

ISSUED 7 MARCH 1985

Approved for public release; distribution unlimited.

LEXINGTON

MASSACHUSETTS

ABSTRACT

A new technology utilizing superconductive components to realize convolvers and correlators that are capable of processing analog signals having bandwidths from 2-20 GHz is being developed. The technology has two key features: (1) low-loss and low-dispersion electromagnetic striplines provide tapped delay on compact substrates; and (2) superconductive tunnel junctions provide efficient low-noise mixing and high-speed sampling circuits. A convolver with a time-bandwidth product of 28 has been demonstrated. Projections indicate that superconductive technology should support analog devices with time-bandwidth products of 1000 or greater.

Accession For	
NTIS GRA&I	<input checked="" type="checkbox"/>
DTIC TAB	<input type="checkbox"/>
Unannounced	<input type="checkbox"/>
Justification	
By	
Distribution/	
Availability Codes	
Dist	
Special	

DDC
QUALITY
INSPECTED
1

AI

TABLE OF CONTENTS

Abstract	iii
1.0 Introduction	1
2.0 Background	3
2.1 Summary of early program results	5
2.2 Related work under other sponsors	6
2.3 Applications and advantages	7
3.0 Progress Report	9
3.1 Junction-ring convolver	9
3.1.1 Delay-line characteristics and device packaging	11
3.1.2 Dynamic range and device efficiency	20
3.1.3 Wideband measurements	25
3.2 Extension of convolver performance	27
3.2.1 Reduction of spurious signal levels	27
3.2.2 Extension of TB product	31
3.3 Time-integrating correlator	34
3.3.1 Integrators/peak detectors	34
3.3.2 Sequential readout	39
Appendix A - Future of Cryogenic Devices for Signal Processing Applications	43
Appendix B - Superconductive Delay-line Technology and Applications	53
Appendix C- Superconductive Convolver with Junction Ring Mixers	63

LIST OF ILLUSTRATIONS

1. Schematic of the superconductive convolver.	10
2. Actual mask layout of the junction-ring convolver. The overall dimensions are 1.0" by 1.6".	12
3. Photograph of convolver substrates and major package piece parts.	14
4. Amplitude-vs-frequency response of the 14-ns-long meander delay line in the convolver.	17
5. Phase-vs-frequency response of the convolver delay line.	18
6. Output waveform of junction-ring convolver with input of two 14-ns-duration gated CW input tones.	22
7. CW output power from convolver as a function of input signal power with fixed reference.	24
8. Output of junction-ring convolver with input of complementary linear chirps.	26
9. Mask layout of short symmetrical couplers.	29
10. Proposed "daisy-wheel" convolver structure.	33
11. Address encoder for superconductive time-integrating correlator.	40

1.0 Introduction

The successful integration of superconductive stripline circuits and tunnel junctions in the same device is yielding programmable analog signal processors with ultrawide bandwidth and important functional capabilities. Configurations of integrated superconductive signal processors and some of their potential areas of application include (1) dispersive delay lines for waveform generation and pulse compression in radar, (2) convolvers and correlators for programmable matched filters in spread-spectrum communication, (3) chirp-transform circuits for spectral analysis, and (4) time-integrating correlators for ultrawide-bandwidth emitter location.

This AFOSR program is a one-staff segment of a multi-staff effort. The other major segments of the effort are supported by the Air Force Lincoln Laboratory line item, by the Ballistic Missile Defense Advanced Technology Center (BMDATC) and the Defense Advanced Research Product Agency (DARPA). The objective of the AFOSR-sponsored segment of the program is to develop convolvers and time-integrating correlators. Unlike our other superconductive structures, these programmable devices require a high degree of integration among the passive stripline and active superconductor-insulator-superconductor (SIS) junction elements. The AFOSR-sponsored portion of the superconductive program has progressed from the development of the separate passive and active superconductive elements through the integration of these superconductive subcomponents to realize, first, a preliminary convolver demonstration and then, an upgraded convolver design with improved characteristics.

In the past year the convolver design has been fabricated and demonstrated with gated-cw tones and wideband chirped waveforms. This device employs a superconductive delay line for the relative shifting of signal and reference waveforms, superconductive mixers for the distributed multiplication, and a low-

impedance output transmission line for summation (integration) of the desired mixing products. These are the essential three functions which are required for convolution. The device was carefully evaluated with cw tones to determine significant device parameters including efficiency, spurious levels and distortions. The results were then compared with our numerical and circuit models which were developed to predict convolver response. The device was then demonstrated as a programmable matched filter using wideband chirped waveforms as the input.

Preliminary design studies have been completed on a time-integrating correlator concept. This device will combine the delay line and mixer structures already developed for the convolver with conceptually new resonator and readout circuits. This device will undergo extensive development during the next two years of the program.

Real-time signal processing bandwidths of 10 GHz and processing gains up to 1000 are projected for the superconductive convolver. The time-integrating correlator, whose interaction is not limited to the physical length of the delay line as in the convolver, will provide processing gains of 10,000 and beyond. The programmable feature of both of these devices will provide the systems designer with the salient attributes of diversity, low probability of intercept and immunity from repeat jamming. Integrated structures of this type will provide real-time signal processing functions with the digital equivalent of over 10^{12} arithmetic operations/sec.

2.0 Background

Radar, communication and electronic warfare systems are often constrained to data rates well below the capabilities of the RF and microwave circuitry by the limitations of their digital data processors. The fundamental task for any signal processor is first to collect data over some time interval and then to analyze that received data, for example by correlation against a known reference or by performing a Fourier transform. It is the goal of this program to develop analog technology that processes the wideband data from a sensor in real time to extract the essential information. This refined data would then be transferred at a substantially reduced rate to a conventional or superconductive digital data processor. Hybrid systems with such analog preprocessors would in consequence have greatly increased capabilities. The potential of such hybrid analog/digital subsystems was described in a recent paper presented at the International Specialists Seminar on Advanced Signal Processing, Appendix A. Reducing the speed requirement for digital processing has immediate and obvious advantages in lowering cost, power, size and weight budgets, and thereby making hybrid systems compatible with such mobile platforms as airplanes and small-land based vehicles. The data reduction afforded by the analog preprocessors has the further advantage of enhancing the robustness of a communication link should it be required to transmit data to another platform (e.g., a central processor).

A variety of functions must be satisfied by the analog signal processing technology. As discussed in the original proposal, these include input, delay, shifting, tapping, multiplication, spatial summation, time integration, and output. Lincoln Laboratory researchers were the first to realize that all of these functions might be achieved in integrated superconductive circuits at bandwidths of 10 GHz and greater. The current program is creating the desired technology. In addition to performing the required analog functions, this

technology also provides a full set of digital logic and memory functions, using compatible devices and processing techniques, which could be incorporated in an ultrahigh-speed processor intermediate between the analog processor and conventional room-temperature circuitry. Until recently, this technology was being aggressively pursued at IBM (and other companies) for computer applications. For reasons related specifically to the application to general-purpose computers, the IBM program was cut back to a much smaller research effort. Those reasons included design difficulties for dense (4K) high-speed memory and loss of momentum to competing high-speed technologies such as advanced silicon and GaAs. However the Josephson digital technology developed at IBM still appears well suited for signal processing applications. Indeed, interest in this particular area is continuing to expand elsewhere within the U.S. superconductive community. Related activities, including mini-refrigerator development for operation at temperatures below 10 K, and searches for a new class of three-terminal transistor-like superconductive device, are being actively pursued by U.S. researchers.

2.1 Summary of early program results

The approach being used in developing superconductive convolvers and time-integrating correlators is to integrate a variety of components via high-quality stripline (or microstrip) links on low-loss substrates. Development under AFOSR sponsorship is progressing in stages, with the first two years being focused on the reliable fabrication of discrete components on low-loss substrates of crystalline quartz and sapphire. Also during this stage of the program a preliminary convolver design was integrated and fabricated on sapphire substrates to demonstrate basic device concepts. The results of this work will be summarized in this subsection. Results on the last phase (third year) of the program will be described in section 3.

During the first two years of the program, superconductive transmission lines, couplers, and tunnel-junction mixers were developed and evaluated at microwave frequencies. The amplitude and phase responses of superconductive transmission lines and taps were extensively studied and modeled. Niobium resonators were fabricated on sapphire, quartz and silicon substrates to evaluate conductor-and substrate-related rf propagation losses. Measurements made at 4.2 K indicated loaded quality (Q) factors of 10^4 and greater for all three substrate materials. Thus niobium and these three substrate materials have sufficiently low RF propagation losses at 4.2 K to support analog signal processing components with signal processing gains of 1000 or greater.

These subcomponents were then integrated on a single sapphire substrate to provide a preliminary demonstration of the superconductive convolver concept. This device employed single-junction mixers which saturated at very low (≈ -80 dBm) output power levels. A new ring mixer was then developed which employs series arrays of superconductive tunnel junctions for the desired mixing interaction. This ring-mixer design was then incorporated in an upgraded

nvolver design to be described in section 3.

2 Related work under other sponsors

Significant advances are being achieved on the passive tapped-delay-line filters being developed for BMDATC. With stripline structures, pulse expansion/compression at 2.4-GHz bandwidths, TB products of 90, and -27-dB peak side-lobe levels are obtained. Swept frequency measurements indicate device amplitude and phase distortions of ± 1 dB and 9° rms, respectively. Measurements on these initial devices indicated significant variations in the group slope between individual devices. This was traced to the presence of air gaps between the two silicon substrates comprising the stripline structure. Improvements in the polishing of the silicon substrates and in the device assembly techniques alleviated this problem.

Two significant advances have been made in extending the length (and hence delay) of the passive filters. A method of stacking multiple series-connected filters in a single package has been developed. Initial demonstration of the structure with a dispersive delay line yielded a 4-GHz bandwidth and a 75-ns dispersion length. To maintain adequate isolation between adjacent line sections, line spacing (s) to substrate height (h) ratios of 3.4 and greater must be maintained. This requirement determines the maximum amount of delay that can be realized with a substrate of fixed dimensions. To increase delay, substrate height must be reduced from the current 125 μm . A method of thinning silicon substrates to thickness of 15 μm and under and bonding the thinned filters to thicker substrates for mechanical support has been achieved. This could yield dispersion times of 200 ns and greater on substrates with current (1-cm) diameters. The technology of superconductive delay lines is more fully explained in an attached paper (Appendix B) which was presented at the 1984 Applied Superconductivity Conference.

2 Dynamic Range and Device Efficiency

The output of the preliminary convolver which was described in previous reports suffered from saturation at very low output power levels. In the design of the device single-junction mixers were employed for the desired nonlinear operation. The maximum output power which can be obtained from an individual junction is limited by the saturation of the tunneling nonlinearity as the RF potential impressed across the superconductive junction is increased above a certain level ($\approx 1\text{mV}$).

The preliminary convolver had limited dynamic range because of this junction saturation. By stacking a number N_j of superconductive junctions in series, one can increase the saturation power P_s by N_j^2 . For example, a superconductive mixer with 4 tunnel junctions in series can have about a 12-dB higher output power level than a single junction mixer.

To increase the available output power and hence dynamic range of the programmable analog signal processing devices, a superconductive diode-ring structure with series junction arrays has been developed and implemented in the present convolver design as shown in Fig. 1. The structure has two RF input ports, a single output port and a dc bias port. Each of its active legs has several superconductive tunnel junctions in series. In device operation, two terminals on opposite sides of each ring are excited by RF inputs from individual proximity couplers. The two couplers are separated by a nominal 90° along the input delay line and ideally, except for a phase shift, carry equal signal (ω_1) and reference (ω_2) components to the mixer terminals. The desired mixing term ($\omega_1 + \omega_2$) between the signal and reference is coherently summed at the lower terminal of the diode ring and directed into a common output line. In addition to the desired mixing term, undesired self-products of the signal ($2\omega_1$) and reference ($2\omega_2$) arrive at the output terminal. However,

which coincide with those from the bends. The response of the quarter-wavelength backward-wave couplers which are employed for sampling the counter-propagating waveforms on the input delay line are within 2 dB of the expected -22-dB coupling strength. The phase response of the couplers tracks fairly well that of the input delay line. Calculations of the magnitude of the reflection at a single tap are -48 db. Means for further reducing these reflections by narrowing the conductor in the tap regions can be implemented. However, control of spurious products and reflections within the mixer rings as well as improved packaging is more important at this time.

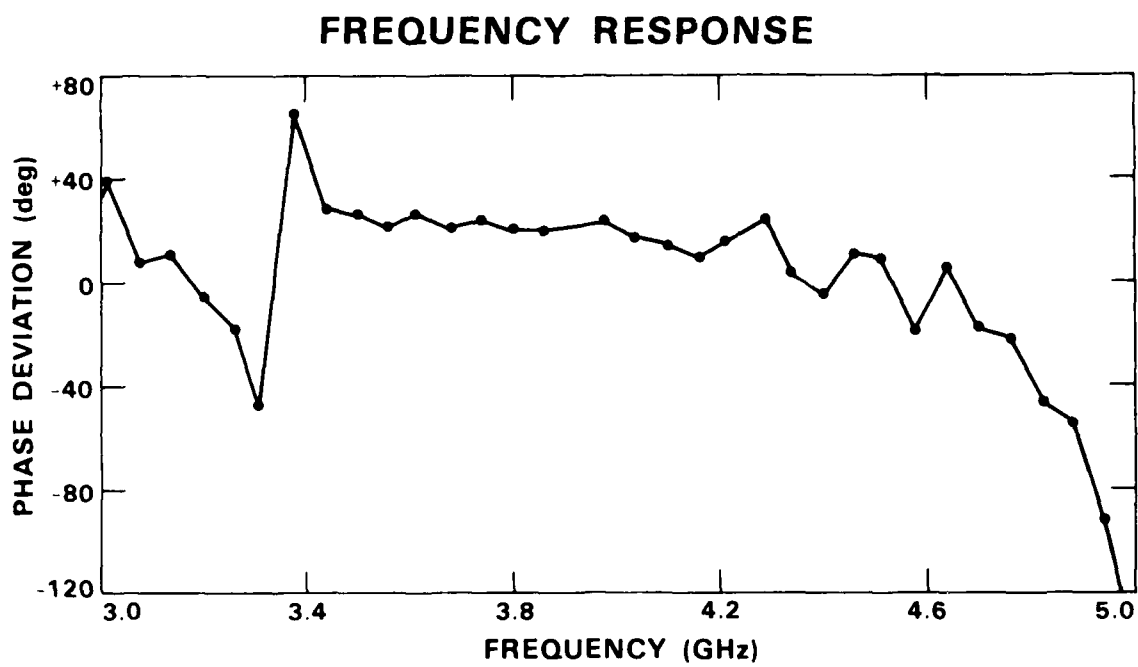


Figure 5. Phase-vs-frequency response of the convolver delay line.

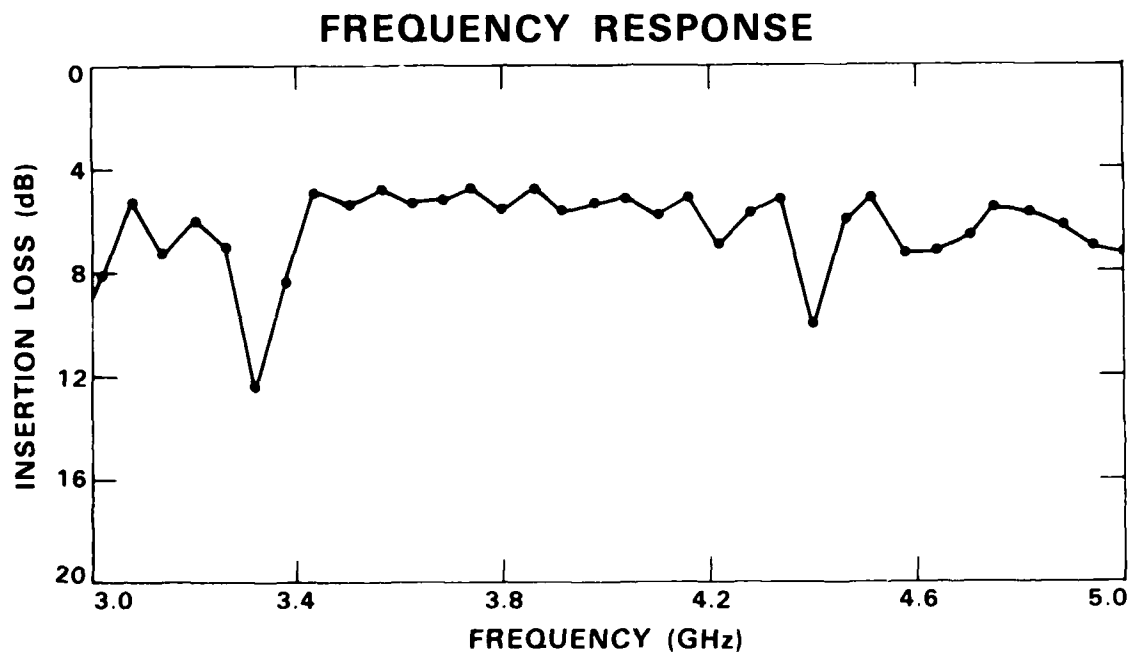


Figure 4. Amplitude-vs-frequency response of the 14-ns-long meander delay line in the convolver.

10 to 20-dB stop bands of the stripline structure. This is because the stripline configuration yields much greater isolation between adjacent line sections than microstrip and provides lower impedance discontinuities at the meander line bends.

The amplitude and phase response of the convolver delay line is plotted in Figures 4 and 5 from 3.0 GHz to 5.0 GHz. About 4 dB of insertion loss and $\pm 10^\circ$ of phase distortion are associated with the test probe and coaxial connectors. The device has a reasonable amplitude and phase response from about 3.4 GHz to 4.8 GHz. The discontinuity which occurs at about 3.3 GHz may be associated with the presence of cavity modes or other packaging problems in the convolver structure. The phase distortion above 4.8 GHz may be associated with both the 2nd stop band and cavity modes. Means of reducing this distortion and extending the bandwidth to a full 2 GHz are being studied. It should be noted that the preliminary convolver with microstrip suffered from 120° of quadratic phase dispersion across a similar bandwidth, and an additional benefit of using stripline is that such dispersion is removed, as can be seen by the nearly flat phase response away from resonances. This improvement is to be expected, since in stripline all of the electric fields are confined to a single dielectric medium.

Empirical evidence exists that when the bend radius of the corner is greater than 3 times the linewidth of the meander line, no significant reflections should be observed at the corners. For the convolver design, curve-radius-to-linewidth ratios of 5.7 were employed, yet reflections of several percent are observed in sections of the delay line indicating nonuniformities in the packaging structure. Forward coupling between adjacent straight-line sections, caused by the anisotropy of the sapphire dielectric and/or dielectric inhomogeneities (e.g., voids between the wafers), can also cause reflections

During device assembly the first sapphire substrate with the major superconductive circuits is placed in a package with RF connectors extending out the bottom side. A second sapphire substrate with another niobium ground plane is placed against the input delay line region of the first substrate to form a stripline circuit. Alignment of these two substrates to each other is determined by slots which have been machined in the base package. A spring insert plate is mounted over the top substrate and 52 beryllium-copper springs are inserted. A central cover plate is then added which compresses the springs and holds the two sapphire substrates in intimate contact. Wire leads are bonded between the device pads and RF connectors for electrical connection. Finally, two additional cover plates are added for mechanical protection of the device.

The meander delay-line design for this device consists of 78 straight-line sections connected by 180-degree bends. Unfortunately, these bends slightly perturb the line impedance and cause reflections. With careful design, the effect of the reflections can be minimized. Because the bends are periodically spaced, these reflections add coherently at certain frequencies and produce stop bands in the transmission response of the delay line. These stop bands occur at frequencies of $N/2\tau_s$ where N is a positive integer and τ_s is the delay per section. The design intentionally places the input frequency band (3-5 GHz) between the 1st and 2nd stop bands. With a τ_s of 0.177 ns, the first two stop bands were expected to occur at about 2.8 and 5.6 GHz. Measurements on the delay-line response indicate a stop band at about 2.9 GHz and a rather complex set of reflections occurring from 5.4 to about 5.8 GHz. The more complicated structure near 5 GHz is attributed to periodic reflections of the taps overlapping with those of the corners. As a comparison, the microstrip meander line of the earlier convolver had 30 to 50-dB stop bands compared to the

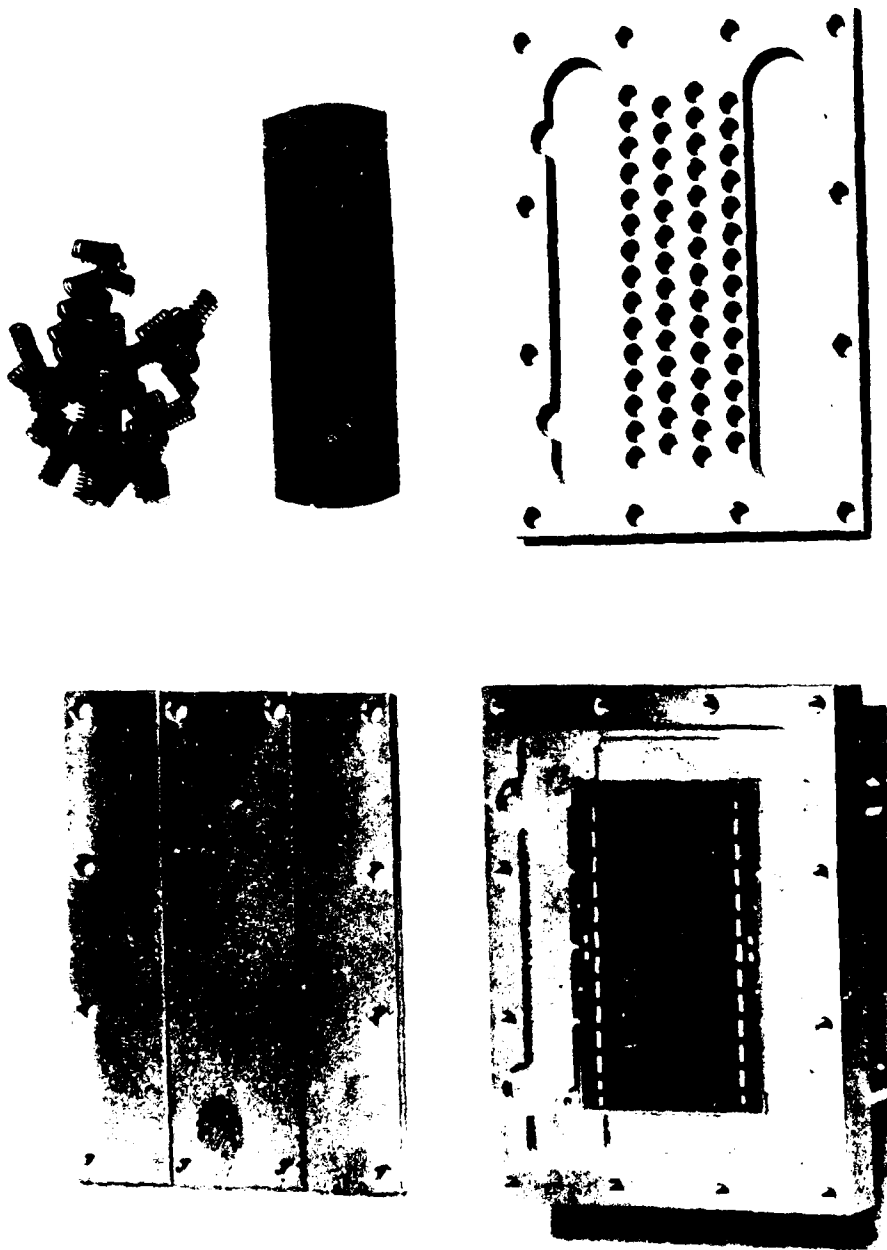


Figure 3. Photograph of convolver substrates and major package piece parts.

11-6-85

the low-impedance ($15\text{-}\Omega$) output line to a standard $50\text{-}\Omega$ impedance. Bias current to optimize the mixing efficiency is distributed from ports B1 and B3 (or B2 and B4). Single-diode-ring test structures are provided at ports D1 and D2. Significant delay line and tap parameters are summarized in Table I.

TABLE I
DIODE-RING CONVOLVER

<u>Parameter</u>	<u>Value</u>
Number of Taps	50
Tap-Pair Periodicity	0.53 ns
Intra-pair Tap Spacing	0.0625 ns
Spacing of Taps along Output Line	0.028 ns
Input Line Impedance	$50\ \Omega$
Output Line Impedance	$14\ \Omega$
Total Interaction Length	14 ns
Time-Bandwidth Product	28
Substrate Size	1" x 1.6" x 0.005"

The major piece-parts for the new convolver design are shown in Figure 3.

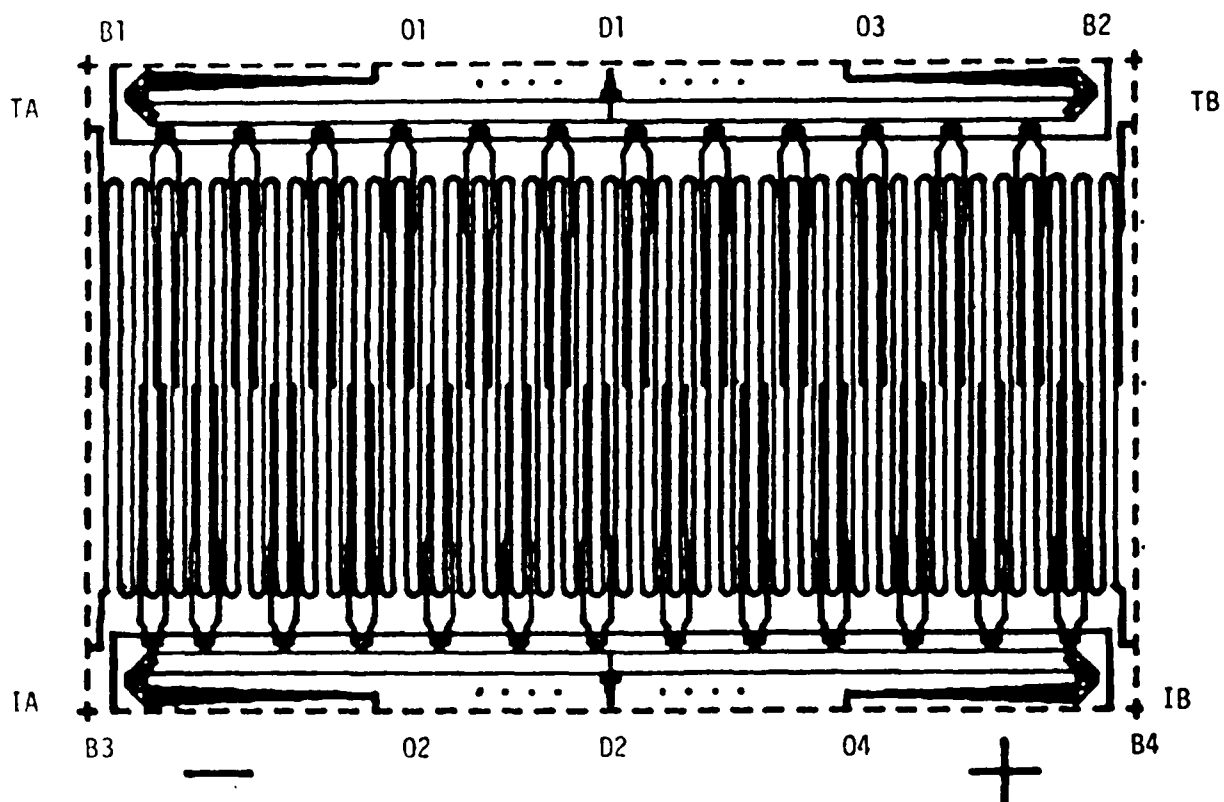


Figure 2. Actual mask layout of the junction-ring convolver.
The overall dimensions are 1.0" by 1.0".

The interaction in the convolver can be expressed by,

$$c(t) = k \int_0^{vT} s(t-x/v) r(t-T + x/v) dx,$$

where k is a scale factor. When $r(t)$ and $s(t)$ are properly timed and also of duration less than T , then the integrand is identically zero outside the limits of the integral, and hence $c(t)$ is precisely the convolution (with a change in time scale and a delay) of $r(t)$ and $s(t)$. Since convolution and correlation are related by a time reversal, a convolver serves as a programmable matched filter when $r(t)$ is a time-reversed replica of the desired waveform.

3.1.1 Delay-Line Characteristics and Device Packaging

The layout of junction-diode-ring convolver is shown schematically in Fig. 2. The central region of the device consists of a meander delay line with proximity taps fabricated on a thin (125- μ m) sapphire substrate. A niobium ground plane is deposited on the opposite side of this substrate. A second sapphire substrate with another niobium ground plane is pressed against the delay line region of the first substrate with a pressure-spring arrangement. This yields a 14-ns-long delay line in a stripline configuration. Signal and reference waveforms are entered into opposite ends (ports IA and IB) of the delay line. Fifty proximity taps sample the propagating waveforms and direct the sampled energy into 25 ring mixers located along both sides of the meander delay line. The response of two test taps can be measured at ports TA and TB. The mixing products formed in the diode-ring structure are collected by two microstrip lines and summed at output ports O1 and O2. Ports O3 and O4 at the opposite ends of the output lines are terminated in their characteristic impedance. A short section of tapered transmission line is used to transform

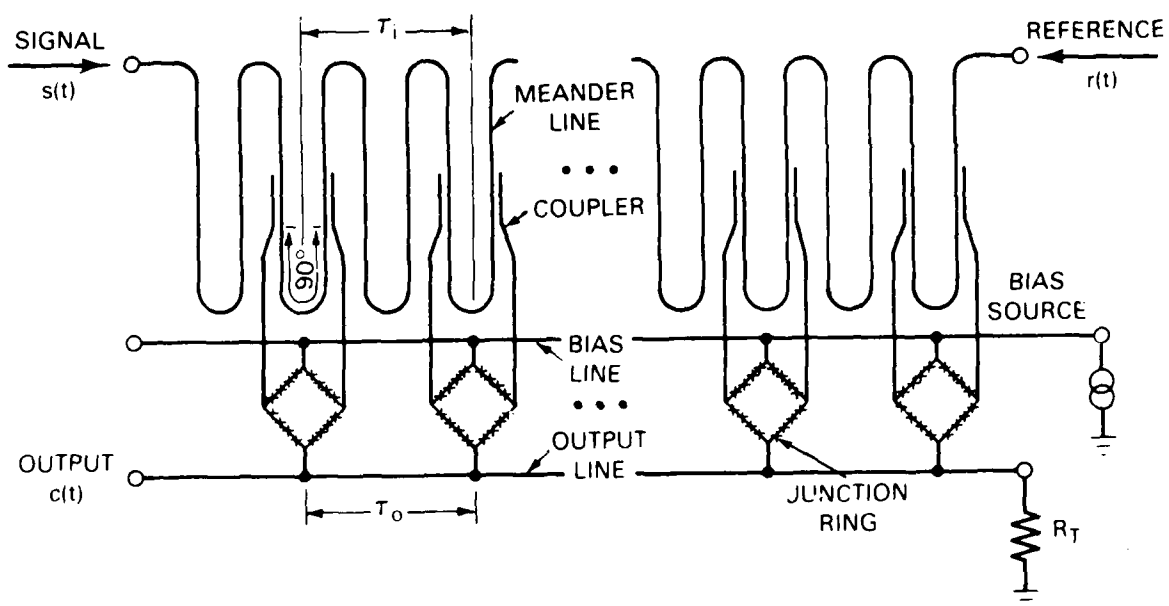


Figure 1. Schematic of the superconductive convolver.

3.0 Progress Report

Significant advances have been made in the development of superconductive devices for analog signal processing applications during the past year. A new convolver design with junction-ring mixers has been fabricated and demonstrated as a programmable matched filter for wideband waveforms. The successful implementation of junction-ring mixers in the device is providing significantly higher convolver output power levels (to -58 dBm), conversion to stripline-type delay structures is yielding reduced phase distortion, and a new package design is providing significantly more reliable device characteristics. Preliminary design work and technology development has been completed on structures which will provide extended convolver TB products in forthcoming devices. Many of the features of the improved convolver design were described in a paper presented at the 1984 Applied Superconductivity Conference, Appendix C.

3.1 Junction-Ring Convolver

Operation of the superconductive convolver is shown schematically in Fig. 1. A signal $s(t-x/v)$ and a reference $r(t-T + x/v)$ counterpropagate along a superconductive delay line having a propagation velocity v and time delay T in the x direction. Samples (delayed replicas) of the two counterpropagating signals are taken at discrete points by proximity taps weakly coupled to the delay line. The sampled energy is directed into superconductive tunnel junctions which produce mixing products. The mixing products are spatially integrated by summing in multiple nodes connected to a short transmission line. The summed energy which appears at the output port of the device includes the desired cross product $c(t)$ and undesired self products of signal and reference as well as higher order terms. Because both of the spatial patterns are moving, there is a halving of the time scale at the output; that is, the center frequency and bandwidth are doubled.

increasingly important to provide electronic countermeasure resistance and low-probability-of-intercept in military communication systems. A 10-GHz-bandwidth convolver for 100-nsec-long pseudo-noise waveforms would provide a robust communication link for 10-MHz data transmission.

Development of a superconductive time-integrating correlator would involve the addition of resonator and readout circuits to the convolver structure. This compact device would be useful in a variety of applications. In a spread-spectrum communication link, it could measure the relative timing between a reference code and an arriving signal, facilitating rapid acquisition of system synchronization. A related application would permit the location of wideband emitters and jammers. This device could also be used to process burst waveforms in small mm-wave radars with necessarily constrained power-aperture products. Yet another application would be as a wideband spectrum analyzer with electronically programmable resolution in an electronic intelligence system or in a wideband warning receiver.

Rapid spectral analysis over an instantaneous bandwidth of 2.4 GHz has recently been demonstrated utilizing superconductive dispersive delay lines in a chirp-transform configuration. Two-tone resolution of 43 MHz and ± 1.2 -dB amplitude uniformity were achieved. The application of superconductive chirp lines to wideband spectral analysis is sponsored by the Defense Advanced Research Projects Agency.

2.3 Applications and Advantages

Analog signal processing components such as charge-coupled devices (CCD) and surface acoustic wave (SAW) devices are often employed as processors to provide real-time processing capability with bandwidths of 10 to 500 MHz. Optical signal processing components are being developed which may extend the bandwidth capability to 2 GHz. But emerging needs are requiring real-time signal processing capabilities in the 1 GHz to 10 GHz regime. Only superconductive signal processing components have the potential of fulfilling this need.

A family of superconductive analog devices is being developed at Lincoln Laboratory. The first device to be developed is a superconductive convolver. It is expected that this device will provide real-time signal processing over 2 GHz to 10 GHz bandwidths with potential signal-processing gains of 1000. The development work on the superconductive convolver will logically feed forward into the development of a time-integrating correlator. Signal-processing gains up to 100,000 are projected for this device. Low-bandwidth versions (< 200 MHz) of both devices exist in acoustoelectric technology.

Applications for a superconductive convolver would include spread-spectrum communication systems in the microwave and mm-wave regions. The use of continually changing codes for spectrum spreading over multi-GHz bandwidths would provide substantial jam-resistance and covertness. It is becoming

the self-products from the two arms of the ring arrive at the output terminal approximately 180° out of phase and effectively cancel each other. Computer simulation indicates that this technique has the potential of providing a 14-dB suppression of this spurious output over the desired 40% fractional bandwidth. Tests on individual junction-ring mixers indicated a nominal 10-dB suppression of this spurious.

The response of the convolver to two 14-ns-long gated-cw tones centered near 3 GHz is shown in Fig. 6. The output waveform approximates the triangular shape expected from the convolution of two nearly square input pulses. The peak power of the output waveform was -62 dBm for input power levels of about -15 dBm. The saturation level P_S of this device is about 18-dB larger than was obtained with the preliminary convolver. Most (12 dB) of this improvement is due to the series junction array with the remaining portion being largely attributed to a reduction in parasitic capacitance.

The efficiency factor for convolvers is commonly defined by

$$F = 10 \log P_O / (P_R P_S) \text{ dBm} \quad (1)$$

where P_S and P_R are the signal and reference input powers and P_O is the output power of the desired product, all expressed in mW. The F factor of the superconductive convolver can be expressed as

$$F = 10 \log (A_i)(A_p)(C_i^2)(M^2)(T_o^2)(R_L), \quad (2)$$

where A_i is the attenuation and signal depletion on the input delay line, A_p is the total loss on the coaxial dewar leads, C_i is the input coupling factor (proximity taps), M is the efficiency factor of an individual junction-ring

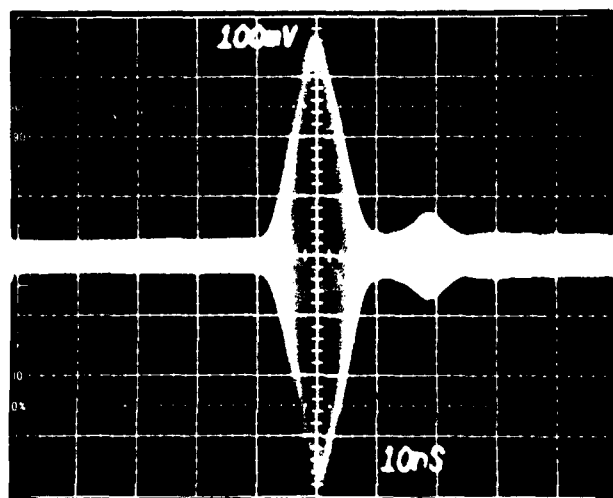


Figure 6. Output waveform of junction-ring convolver with input of two 14-ns-duration gated CW input tones.

mixer and R_L is the load (output transmission line) impedance. Predictions for A_i , A_p and C_i are readily obtained from standard transmission-line models and confirmed with standard RF insertion-loss and resonator Q measurements. Circuit models have been developed to predict mixer efficiency M and the output circuit transfer function T_o . RF measurements on individual SIS diodes confirm the predictions for M . Predicted and measured values for the convolver design are listed in Table II. The considerable uncertainty in the measured values for A_i and C_i is due to frequency ripple in the measurement of the proximity coupler response and the cumulative effects of reflections both within the meander line and from the coaxial-line terminations of the test set.

TABLE II
PREDICTED AND MEASURED PARAMETERS FOR SUPERCONDUCTIVE CONVOLVERS WITH
JUNCTION-RING MIXERS.

<u>PARAMETER</u>	<u>PREDICTED</u>	<u>MEASURED</u>
A_i	≈ 1 dB	-2 ± 2 dB
A_p	- 6 dB	-5 dB
C_i	-24 dB	-23 ± 3 dB
M	40 A/W	-
MT_o	200 A/W	100 A/W
F	-28 dBm	-32 dBm

A plot of CW output power from the 50 tap convolver as a function of input signal level is shown in Fig. 7. For this measurement, the reference power level was held at a constant -10 dBm.

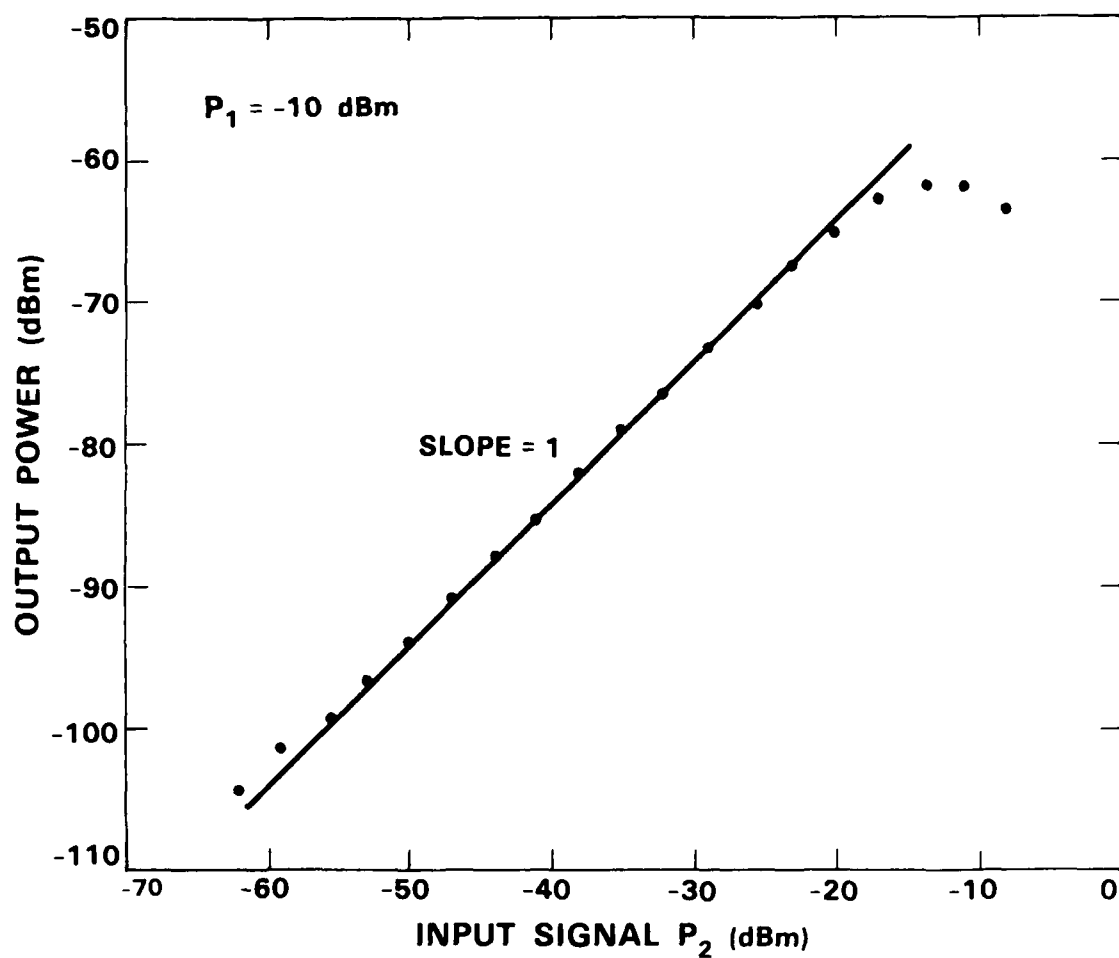


Figure 7. CW output power from convolver as a function of input signal power with fixed reference.

3.1.3 Wideband Measurements

The junction-ring convolver has recently been demonstrated as a programmable matched filter for near 1-GHz-bandwidth chirped waveforms. Input waveforms consisting of a flat-weighted upchirp and a complementary downchirp were applied to the signal and reference ports of the convolver. The waveforms were generated by two of the superconductive tapped-delay-line filters being developed for the BMDATC program. The waveforms had chirp slopes of about 62 MHz/ns and were effectively truncated to instantaneous bandwidths of about 0.85 GHz by the 14-ns-long interaction length of the convolver.

The resultant output waveform shown in Fig. 8 has a bandwidth of about 1.7 GHz. Use of flat-weighted chirps with adequate TB products should yield a $(\sin x)/x$ response with a null-to-null width of 1.2 ns and peak relative side lobes of -13 dB. A null-to-null width of 1.5 ns was observed with excessively high -7-dB side-lobe levels. These distortions are attributed primarily to mixer products produced from undesired leakage and electromagnetic feedthrough of input signal onto the output line. In the next stage of the device development, the spurious sidelobe levels will be reduced by improved design of the input and output transmission-line circuits.



Figure 8. Output of junction-ring convolver with input of complementary linear chirps.

3.2 Extension of convolver performance

Design studies and experiments were carried out to evaluate steps which could be taken to reduce spurious levels in the current convolver design and to extend TB products in future designs.

3.2.1 Reduction of spurious signal levels

To realize our goal of a practical signal processing device, the linear dynamic range of the convolver must exceed its signal processing gain. The dynamic range of a convolver is defined as the ratio of the output power level at which the device begins to saturate (e.g., where F is changed by 1 dB) to the power level of the spurious signals or system thermal noise floor kTB , whichever is greater. With current amplifier technology, the thermal noise floor at 4 GHz bandwidths is limited to about -78 dBm. Spurious signal levels vary considerably across the operating frequency band but in general are above the thermal noise floor and hence are the limiting factor in convolver operation.

The junction-ring configuration, as do other balanced or doubly-balanced mixer designs, cancels the even-harmonic signal ($2\omega_S$) and reference ($2\omega_R$) self-product terms but can do little for many of the undesired odd-harmonic terms ($3\omega_S - \omega_R$, $3\omega_R - \omega_S$, etc). These undesired cross products have the potential of being effectively suppressed because the desired convolution product has a relatively slow phase progression on the output line compared with the undesired mixer products; thus the spatial summation of the undesired products tends to average to zero. However, the taps in a superconductive convolver are discrete, and simple periodic tap configurations will not only sum the desired product, but deliver substantial output at certain frequencies for the undesired products as well. A tap placement scheme with a pseudorandom

spacing (or chirped spacing) along the meander delay line has been studied and can suppress these undesired mixing products by $1/\sqrt{N}$ (or $1/N$) where N is the number of tap pairs. This has not been implemented in the current convolver design, but may be essential in future designs.

The desired (>14 dB) suppression of signal and reference self-products has not been realized in the junction-ring convolvers fabricated and evaluated to date. This has been traced to three probable causes: (1) The response of the current coupler configuration is dependent on the direction of propagation on the input delay line and hence true balanced inputs are not delivered to the two input ports of the convolver; (2) when the impedance of the tunnel-junction mixers is not properly controlled, severe impedance mismatches can occur at the coupler/mixer interface which results in multiple reflections in the coupler and phase distortion of the input signals; and (3) measurements indicate that excessive (≈ -30 dB) coupling of input signal onto the output summing line and bias line is occurring. This causes adjacent mixers to interact with each other, providing another potential source of phase distortion.

A new coupler design, shown in Fig 9, has been examined as a means of resolving the problems associated with the coupler/mixer imbalances and impedance mismatches. In this design the couplers are symmetrical with respect to both the mixer input ports and input delay line. This configuration is expected to deliver equal samples of the signal (or reference) waveforms to both input ports of the mixer. The couplers themselves and the RF leads to the ring mixer are deliberately kept short ($\ll \lambda/4$) so that the coupler is effectively a lumped element (capacitor) and the effects of line reflections become substantially less of a problem. This design does require additional bends in the input delay line and possibly compensation for the frequency-dependent

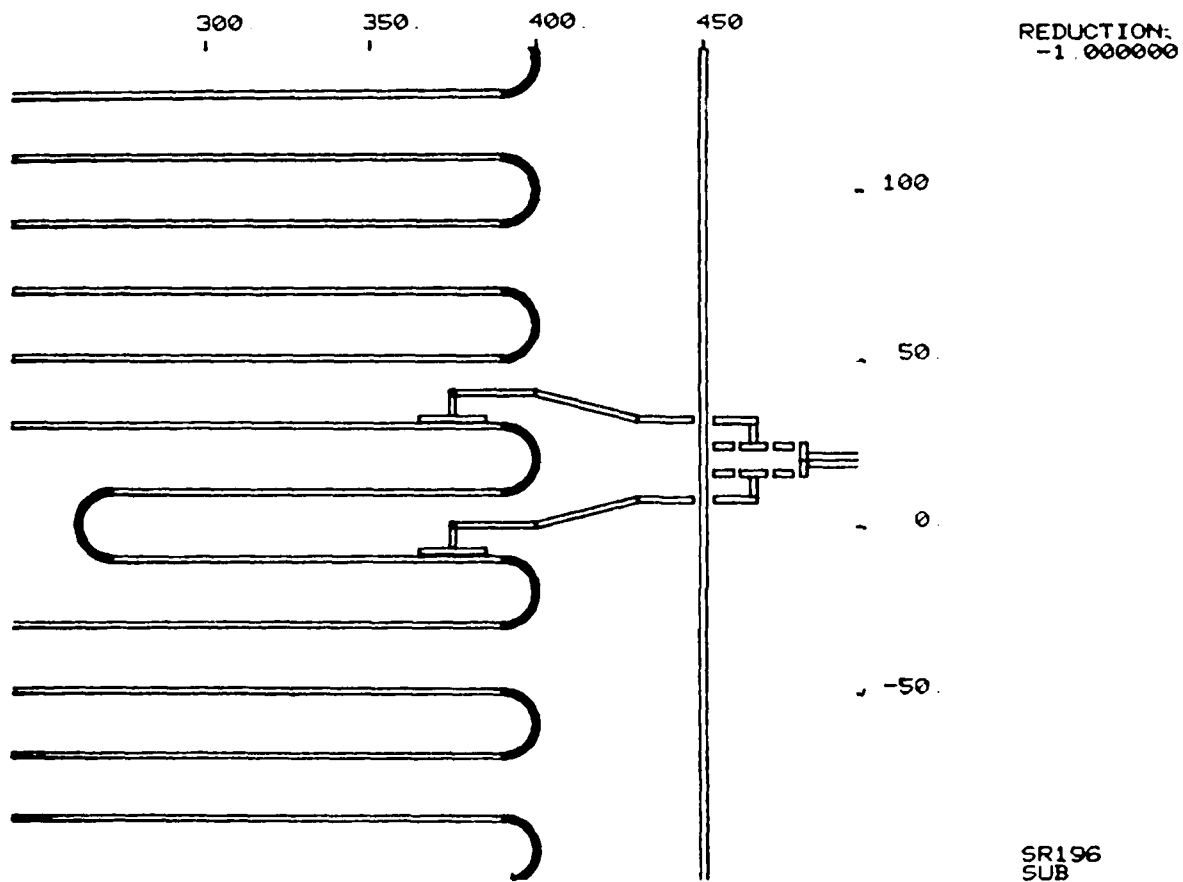


Figure 9. Mask layout of short symmetrical couplers.

response of the coupler. Couplers of this type are being fabricated and will be evaluated for possible implementation on the next convolver design. An alternative approach is to add a resistive pad in series with the superconductive (niobium) coupler so that the propagation path has several dB of loss and multiple reflections are more rapidly attenuated.

Undesired RF coupling between the input delay line and the output line can be reduced by physically increasing the line-to-line separation or by conversion from the current microstrip structure to stripline. The implementation of high-pass filters at each mixer has been explored as an alternative approach. In terms of simplicity and the conservation of substrate area, the first approach appears to be the most desirable at the present time.

3.2.2 Extension of Time-Bandwidth Product

The maximum potential signal-processing gain of an analog device is equal to its time-bandwidth (TB) product, where T , the interaction time, is the total delay length of the device over which the waveform is adequately sampled and B , the bandwidth, is limited to the frequency range over which the amplitude and phase response of the device is well behaved. Adequate sampling requires that the time delay between any two complex samples of the waveform not exceed $1/B$. The convolver design described in this report has a maximum tap-delay spacing of about 0.47 ns for a potential bandwidth slightly greater than 2 GHz and a delay time of about 14 ns; thus it has a nominal TB product of 30.

Progress has been made in both the technology required to realize longer interaction lengths and in conceptual designs which incorporate substantially larger numbers of composite tap/mixer sections.

The greatest technical stress in extending the time-bandwidth product of the convolver is in increasing the interaction length to well beyond the current 14 ns while keeping amplitude and phase characteristics under even tighter control. To minimize distortions associated with adjacent line coupling, the closest transmission line sections must be spaced at least 3.5 times the thickness of the dielectric substrate. Therefore, dielectric thickness determines the spacing between lines and hence the maximum delay per unit of substrate surface area. We are currently employing substrates of 125- μm thickness. As mentioned earlier, low-loss silicon substrates that have been bonded to carriers and thinned to 15 μm are currently being developed under AF Line sponsorship. We expect high-quality thin dielectrics to be available for device development during the next phase of the AFOSR program. This will allow the fabrication of programmable devices with interaction lengths of 200 ns on a single, 5-cm-diameter substrate. Even larger delays could be realized by

tacking multiple wafers with the packaging designs currently under development or the BMDATC program.

A "daisy-wheel" delay line structure, shown in Fig. 10, has been conceived and investigated as an alternative to the present "meander-line" structure. The modified structure will maximize the utilization of the surface area of the round substrates. A convolver with a TB product of 100 can be fabricated on 25- μ m-thick, 7.6-cm-diameter substrates. Thinner substrates would allow even greater circuit density and correspondingly larger convolver TB products. To have a TB product of 100, a like number of mixers is required. The mixers and output lines will be located around the outer edges of the "daisy-wheel" design, and refinements demonstrated for spurious suppression on the current meander configuration will be incorporated into the "daisy-wheel" configuration.

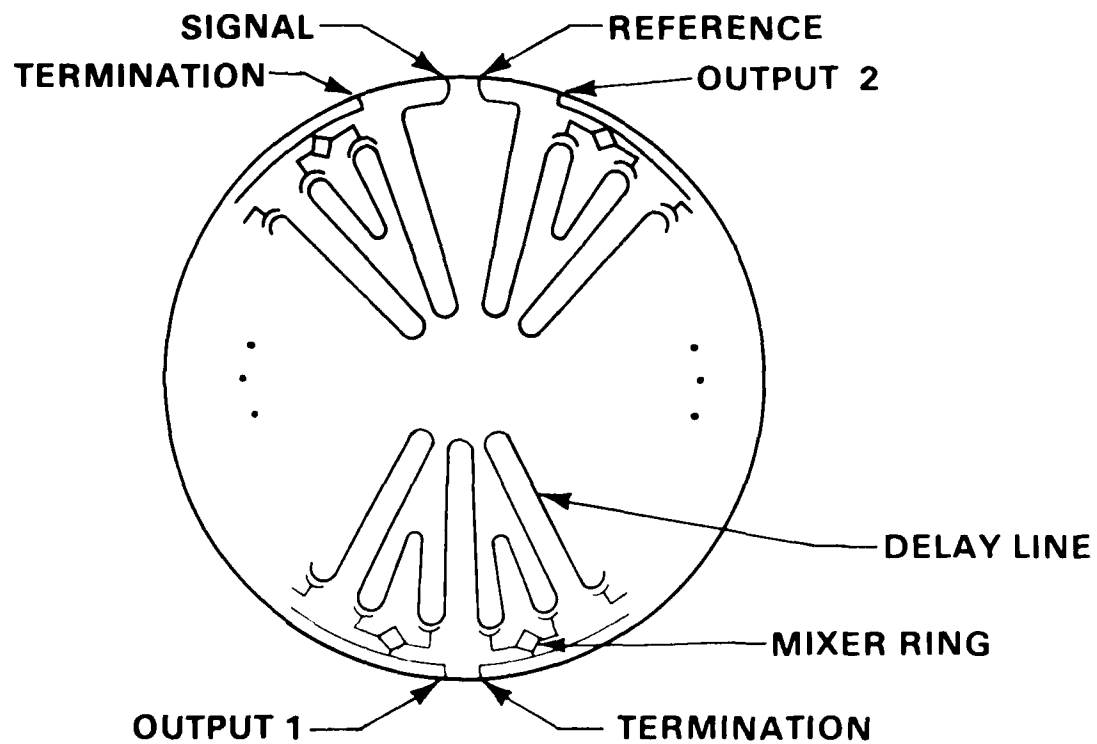


Figure 10. Proposed "daisy-wheel" convolver structure.

3 Time-Integrating Correlator

The time-integrating correlator requires three new components in addition to those already developed for the convolver. These are integrators, peak detectors, and an output multiplexer. New components to fulfill these functions have been conceived and analyzed. These components are expected to provide substantial functional improvements over the components originally proposed. The next step will be to fabricate these devices and evaluate both their individual performance and their response in an integrated structure.

3.1 Integrators/Peak Detectors

In the original concept, the integrators were stripline resonators operating at a frequency of ≈ 2 GHz and with required quality factors Q in excess of 10^4 . For a bandwidth comparable to this resonant frequency, the time-bandwidth product, and hence the potential signal-processing gain, is ≈ 50 dB. The use of very high- Q resonators posed several technical challenges. These include the need for sufficient coupling between the resonators and the peak detectors and the SIS mixers to provide an adequate signal without excessive loading which would degrade the Q ; the requirement for negligible unwanted coupling between resonators; and the need for precise uniformity in the resonant frequencies. Of these three requirements the need for precise uniformity ($>1/Q$) of the resonant frequencies appeared to be the most difficult to achieve.

Josephson junctions will switch prematurely out of the zero-voltage state when the current through the junction is smaller than the "true" critical current because of either thermal or external noise. The noise in the measured critical currents is typically 5 μ A at 4.2 K. For such a junction to serve as a peak detector with a dynamic range of 40 dB, therefore, ac signal amplitudes of 10 μ A are required.

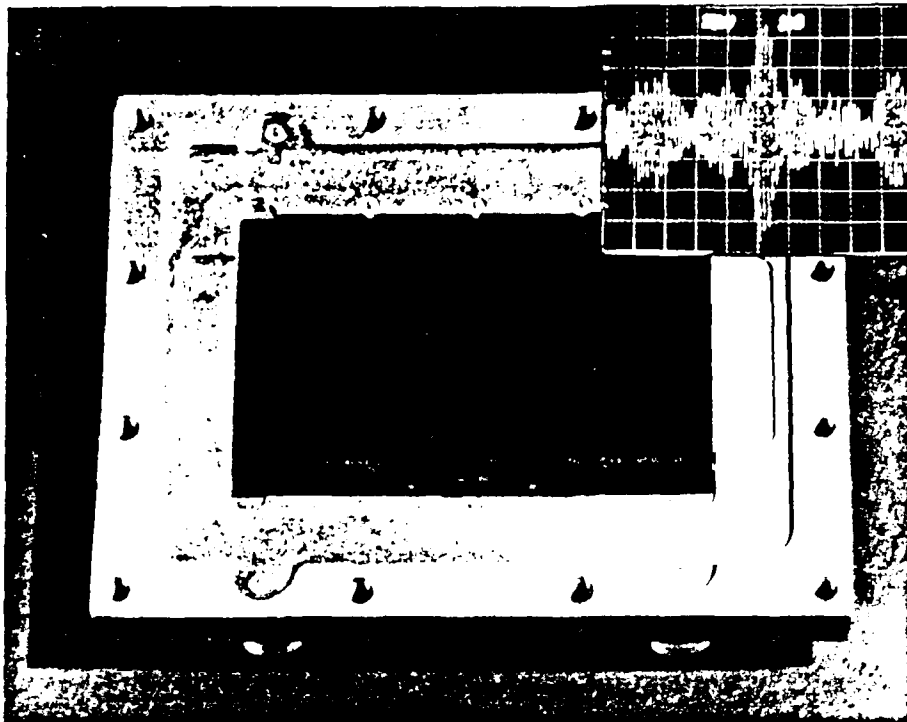


Fig. 3 Photograph of a superconductive convolver fabricated on 2.5-cm by 4-cm sapphire substrate. Inset shows wideband (≈ 1.6 GHz) compressed pulse output.

The projected bandwidths for several analog signal processing devices are shown in Fig. 4. Charge-coupled devices (CCDs) occupy a bandwidth regime which is being compressed on the bottom by digital systems and on the top by acoustic devices. Acoustic devices for signal processing exist in well-engineered forms and currently operate near their projected bandwidth limits of several hundred megahertz. Optical and superconductive devices exist in a less advanced state of development, but the superconductive devices already provide considerably larger bandwidths than available from acoustic devices. The signal processing gain available from most of these analog devices will range from somewhat under 10^3 to 10^4 .

1.3 DIGITAL SIGNAL PROCESSING

In the past year we have seen the discontinuation of several large commercial efforts to build digital circuits and a general purpose, mainframe computer with Josephson technology. A development effort at IBM extended over more than a decade and brought forth many exciting new developments in technology, circuit concepts, cryogenics and systems engineering (7). The Josephson technology itself failed, largely through a lack of useful power gain, to provide adequate design margins for the essential high-speed memory with the required extremely low error rates. This should not be viewed as a fundamental limit, but rather an inability to reach the commercial marketplace in a timely fashion. Other cryogenic concepts and technologies may one day provide this gain and a superconductive mainframe computer effort may be reinstated.

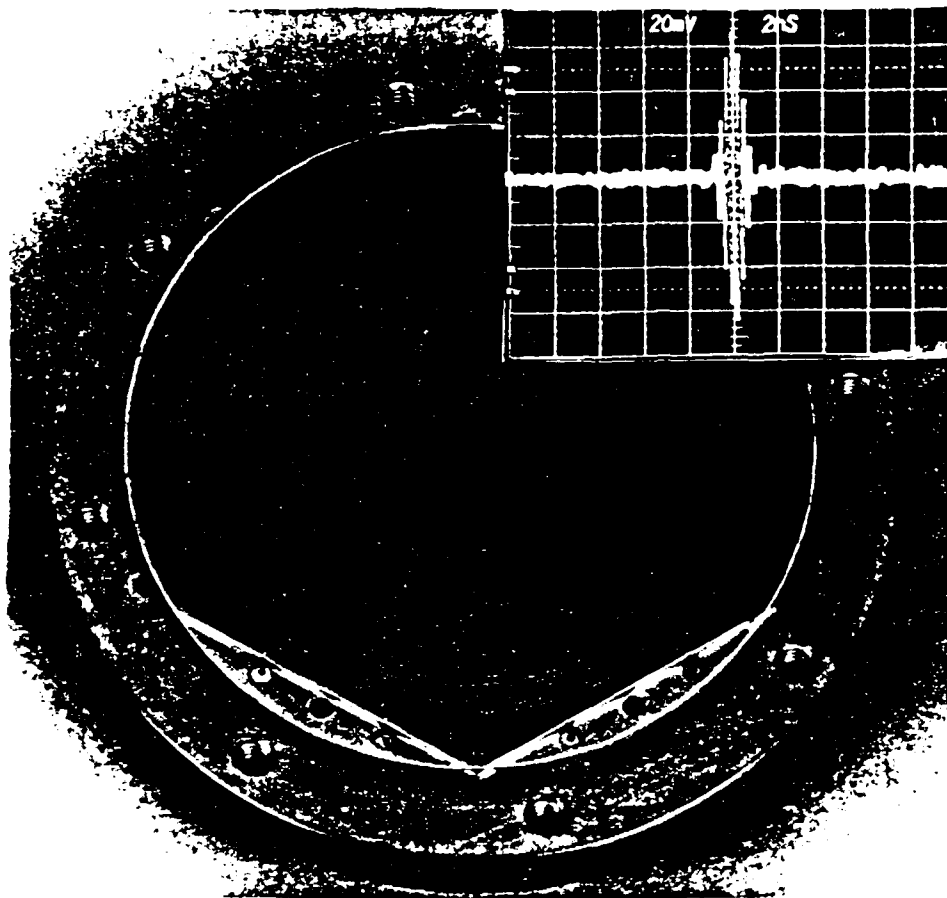


Fig. 2 Photograph of superconductive tapped delay line fabricated on 5-cm-diameter silicon substrate with Hamming weighting. Inset shows compressed pulse output of this 2.3-GHz bandwidth, 37.5-ns dispersion device.

response is shown in the inset in Fig. 3. The high spurious levels are due to the formation of undesired products in the mixing interaction. With a dynamic reference, these devices can provide programmable matched filtering. Alternatively, a time integrating correlator can be realized by replacing the summation output lines with individual superconducting resonators, and by using superconductive logic to provide the readout function. Signal processing bandwidths of 10 GHz and TB products of 1000 and more are projected for both the passive and programmable superconductive devices.

Although the time-integrating devices provide a convenient time buffering of the data, many analog signal processing devices transform signals from one parameter range (e.g., frequency) to another (e.g., time) without providing any significant reduction in data. The output of devices such as the pulse compressor and convolver must be sampled at their full bandwidth and decisions be made with high-speed digital logic. Circuits to perform these functions can be provided very conveniently by superconductive technology. Several research laboratories (5), (6) are developing analog/digital (A/D) converters with superconductive circuits. Three-bit accuracies with about a 0.5-GHz analog bandwidth have been demonstrated, with the primary limitation being the lack of an adequate sample and hold.

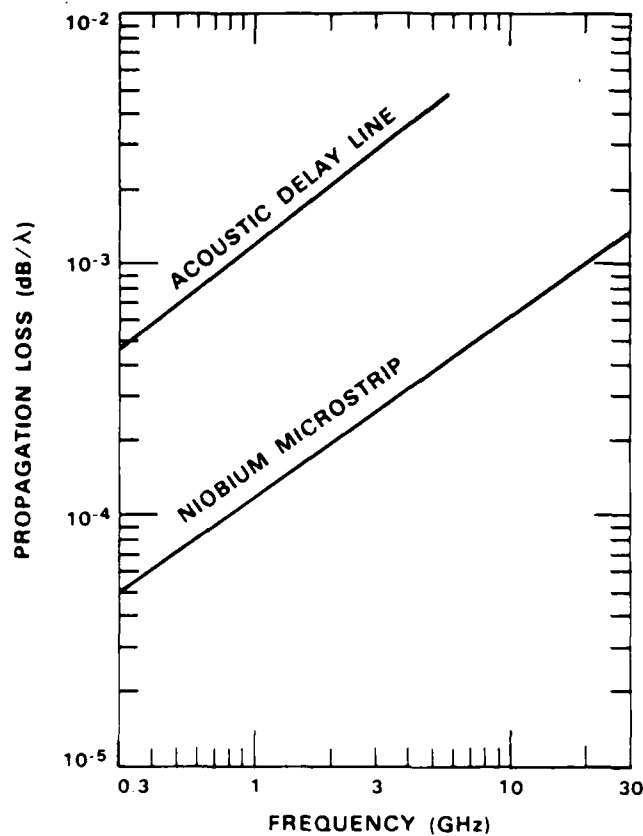


Fig. 1 Propagation loss per wavelength of delay for acoustic and superconductive delay lines.

be about three orders of magnitude larger. The same superconductive technology provides dense interconnects for signal transmission in digital circuits.

A pulse expander/pulse compressor has recently been realized at Lincoln Laboratory (3) by integrating superconductive transmission lines and proximity couplers on a 5-cm-diameter silicon wafer, as shown in Fig. 2. The tapped-delay-line structure currently provides a signal processing bandwidth of 2.3 GHz and a TB product of 86 with measured amplitude ripple of 1.5 dB and phase deviations from quadratic of 9 degrees rms. The compressed pulse for a Hamming-weighted linear-frequency-modulated chirp waveform is shown in the inset in Fig. 2; it has a respectable peak-to-side-lobe level of 27 dB. Side-lobe levels of -40 dB are expected in refined devices.

By adding to a tapped delay line structure both mixers for multiplication and a microstrip line for spatial summation, the generic functions of convolution or correlation can be realized. Such a programmable device is being developed at Lincoln Laboratory (4). A photograph of a superconducting convolver is shown in Fig. 3. A meander line provides delay, 50 proximity couplers provide sampling, 25 junction-ring mixers provide local multiplication and two short transmission lines provide summation (or integration) and output. This device has recently been demonstrated with both gated-cw input tones and wideband (≈ 1 GHz) chirped waveforms. The wideband output

duplicate the desired signal-processing function. Such integrated components must simultaneously perform multiple functions such as delay, distributed multiplication and summation with often very stressing requirements (1). A list of these functions, along with the most stressing requirements and the superconducting component which can fulfill the particular function, is given in Table 1. Some of the functions, notably multiplication and readout, may be provided by cooled semiconductor circuits with the potential for higher dynamic ranges but at the cost of greater cooling requirements.

TABLE I Functions Required for Analog Signal Processing

Function	Requirement	Component
Delay	Low Dispersion Low Loss Compactness	Stripline
Tapping	Accurate Weights	Proximity Coupler
Multiplication	Adequate Dynamic Range	Mixer
Spatial Summation	Phase Coherence	Microstrip
Time Integration	Adequate Storage Time	Resonator
Readout	Sensitivity	Logic

The most significant figure of merit for the signal processing system is processing gain. This is defined as the improvement in the signal-to-noise ratio of the output signal relative to the input signal. The maximum potential processing gain of a device is equal to its time-bandwidth (TB) product, and in well-engineered integrations of device and peripheral electronics this maximum processing gain can be realized to within about 1 dB.

One of the most stressing requirements of analog signal processing is the need to provide for temporary storage of several thousand wavelengths of analog signal without excessive phase or amplitude distortion. Acoustic technology has filled a substantial niche in signal processing applications because acoustic waves can provide low-loss delays with small phase distortions (2). Superconductive technology can provide low-loss transmission lines on dielectric substrates with much shorter delays than available from acoustic devices but with at least an order of magnitude increase in bandwidth (1). The loss per wavelength of delay for both structures is plotted in Fig. 1 as a function of frequency. Projected losses are shown for Rayleigh waves on lithium niobate at 300 K and for niobium microstrip lines at 4.2 K on 25- μ m-thick, low-loss substrates. Comparable losses with normal metal transmission lines at 4.2 K would

FUTURE OF CRYOGENIC DEVICES FOR SIGNAL PROCESSING APPLICATIONS*

S. A. Reible
Lincoln Laboratory, Massachusetts Institute of Technology
Lexington, Massachusetts 02173 - 0073

1.1 INTRODUCTION

The principal advantages of superconductive circuits in both analog and digital applications are high switching speed (hence large bandwidth), low propagation loss and low power dissipation. In spite of rapid advances in semiconductor and other competing technologies, superconductive circuits continue to maintain a nominal order-of-magnitude advantage in speed. Superconductive circuits operate at very low power levels, but the need to provide a cryogenic environment eliminates most of their advantage when comparing total power requirements. However, the low power dissipation translates to a potential advantage in circuit density.

The distinct speed advantage of superconductive technology will find its greatest usage in real-time signal processing. Potential applications include: correlation and analysis of wideband signals, matched filtering, and integrated-focal-plane-array processing. Bandwidths of 10 GHz and signal processing gains of 1000 and beyond are projected for superconductive correlators and other signal-processing devices. Direct signal processing of gigahertz-bandwidth signals will allow very high resolution and possibly even three-dimensional details to be determined for identification and classification purposes at high frame rates. Furthermore, because many future systems will require cryogenic sensors (e.g., for mm-wave or infrared radiation), the superconductive circuits can be integrated into the sensor module with little additional investment in power or space. Hybrid analog/digital signal-processing architectures implemented with cryogenic circuits will extend the available processing gain in noisy environments.

This paper will describe some of the essential functions required for analog and digital signal processing. Cryogenic circuits can fulfill all of the required functions for signal processing, often with more than an order of magnitude increase in bandwidth capability over that which is available from existing room-temperature circuits.

1.2 ANALOG SIGNAL PROCESSING

To perform analog signal processing it is necessary to configure a structure or a collection of components whose equations of motion

*This work was sponsored by the Department of the Air Force, the Department of the Army, and the Air Force Office of Scientific Research.

Appendix A

Future of Cryogenic Devices for Signal Processing Applications.

Presented at the International Specialists
Seminar on Advanced Signal Processing,
Warwick, England, 1984

translates into maximum operating margins. Thus, we believe that this design can be successfully implemented using the existing Nb-Nb₂O₅-Pb fabrication capability. Also, it can be fabricated either on the same substrate as the analog portion of the correlator or could be fabricated on a separate substrate and interfaced to the analog circuit inductively.

the address line connected to that channel and is encoded by the address encoders according to its binary address. Superconducting quantum interference devices (SQUIDs) latch into the voltage state in response to the current diverted by the switching of the peak detector. The function of the complement address gate is to ensure that the state of the address gate does not change in the event a second threshold detector switches until the first address is read out and the gates are reset.

For applications which require readout of the contents and address of only a single channel corresponding to the correlation peak, minimal additional logic is required. If the application requires output from more than one channel, additional logic is required and can be implemented either on or off chip, depending on the systems requirements. For example, the maximum performance could be achieved (at the expense of the maximum complexity) by shifting the contents of the address gates into a superconducting shift register, along with the contents of a clock register. Josephson logic would then automatically reset the address gates. This readout operation could be achieved at a rate much faster than the 100 MHz quoted earlier, so that the likelihood of losing any data when channels have near-equal contents could be kept small. Alternatively, the clocking and reset operation could be accomplished using room-temperature electronics.

This content-sequential readout scheme is especially well suited for implementation with Josephson logic, because it exploits threshold-sensitive latching logic. The serial fanout allowed by using magnetically coupled Josephson logic allows all $2n$ address gates to be driven with each address line and also allows many inputs to be coupled to a single OR gate. This design uses a minimal number of logic gates, thus maximizing fabrication yield. The use of a single level of logic, provided by the multi-input OR gates and serial fanout,

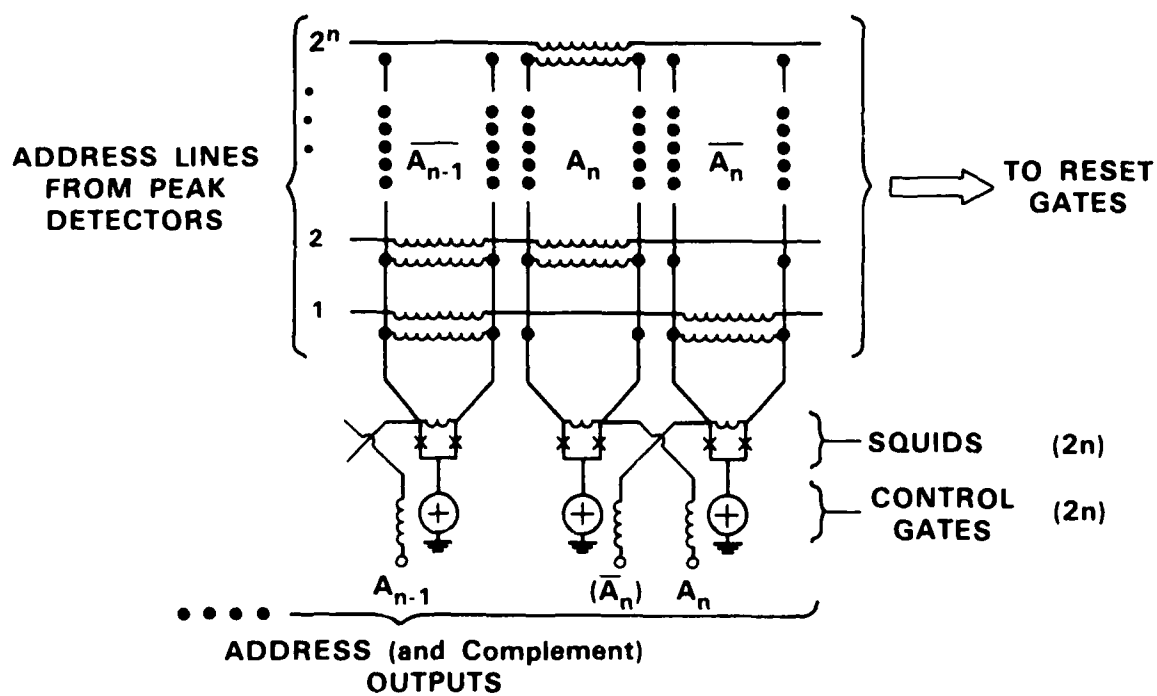


Figure 11. Address encoder for superconductive time-integrating correlator.

determined to 1/100 of a cycle, or 3.6° . This phase uncertainty is commensurate with the amplitude uncertainty for a near full-scale signal imposed by noise in the peak detectors.

On the other hand, a lower Q reduces the precision of the amplitude measurement, since the amplitude decays by $\approx 1/Q$ per cycle. However, the precision is still better than 1% for a Q of ≈ 400 , and substantially greater precision could not be achieved anyway because of the precision of the peak detectors. Thus, with very little sacrifice in amplitude precision, the new design has the potential for providing useful phase information which was not possible with the original design.

3.3.2 Sequential Readout

Every data frame output by the correlator may contain data from up to approximately 1000 individual channels, each corresponding to a slightly different time delay. If each channel were to be serially accessed, the output data rate would be about 100 MHz. However, for most applications, particularly those related to emitter location or communications, only those channels with the largest contents are of interest. A readout scheme which addresses the channels in order of magnitude of their contents (content-sequential order), rather than in address-sequential order, is desirable for these applications, since it would automatically perform the function of locating the correlation peaks and could reduce the output data rate to below 1 MHz.

The heart of the Josephson readout circuit is an address encoder, consisting of 2^n OR gates, which allows the encoding of an n -bit address and its complement. Each OR gate has 2^n inputs - one for each channel - of which the half corresponding to the binary bit of the address (or its complement) are coupled by a mutual inductance. This is shown schematically in Fig. 11. When the peak detector in one of the integrators switches, current is diverted down

the bandwidth of the TIC. If the resonator frequency is smaller than the TIC bandwidth, then undesired products also occur at negative frequencies, and if the resonator frequency is smaller than half the TIC bandwidth, undesired products also occur at the negative of the resonator frequency. This results in an additional implementation loss of 3 dB, since the noise input to the resonator is doubled. While the loss of 3 dB of signal processing gain may seem trivial when compared to the overall potential gain of 40-50 dB associated with the large TB product, it can still be translated into the need for twice as much signal power, which ultimately requires a larger transmitter or antenna, and thus is unacceptable.

This source of implementation loss can be eliminated by using the following double-heterodyne technique. The signal and reference are offset by a frequency greater than half their bandwidth, as in the original design. However, the integration is not performed at this frequency. Rather, the mixer output is first filtered through a narrow bandpass filter centered on the offset frequency, and then mixed down to a lower frequency for integration.

A comparison of the new design with the original design is interesting. The use of an additional mixing stage and filter has in a sense solved the problem of achieving uniformities of a few ppm in resonator frequencies by dividing it up into two stages, each of which has only to achieve uniformities of the order of a part in 10^3 . Moreover, the concern about stray coupling between resonators is relieved to a very great extent.

The new design has an additional potential signal-processing benefit. The peak detectors can only switch during the portion of the cycle when the phase of the signal is near $\pi/2$. If the timing of a peak detection is achieved using, for example, a 2-GHz clock, then the relative phase of the signal can be

loss. We have concluded that a 20-MHz, $Q = 400$ lumped-element resonator, which would have the same integration time as the originally proposed 2-GHz, $Q = 4 \times 10^4$ stripline resonator, is a viable approach.

The move to low Q removes the need for very low loss dielectrics, permitting the use of anodized Nb (Nb_2O_5) which has a measured loss tangent of 2×10^{-3} and a specific capacitance of 6000 pF/mm² at a thickness of 450 Å. In addition, this material has a low defect density. Thus, it is anticipated that resonators using $L \approx 10000$ pH and $C = 6000$ pF can be made with $Q \approx 500$ and in an area of ≈ 2 mm².

The gain factor of $Q^{1/2}$ which was obtained in the high- Q stripline design is inadequate for this new low- Q design if the noise level in the peak detector and the mixer output levels remain unchanged. The loading of the resonator, however, depends not only on the coupling strength but also on the ratio of the mixer output impedance and the resonator characteristic impedance. For our new design, the characteristic impedance $Z = \sqrt{L/C}$ is very low, 1.2 Ω . This means that it can be strongly coupled to the mixer output without excessive loading so long as the mixer output impedance exceeds 500 Ω , resulting in a gain factor of Q . Thus, the absolute resonator current levels are comparable to those obtained in the original design and should be well matched to the requirements of the peak detectors. While a mixer design has not been finalized, the high output-impedance requirement does not appear to be a major problem.

We originally suspected that the bandwidth of the TIC might be limited to a value no larger than the resonator frequency. The move to very much lower frequencies thus demanded a more rigorous analysis of this potential problem.

The desired product between the signal and the reference falls at the resonator frequency, but the undesired products of the reference and the noise fall in a broad band which is centered on the resonator frequency and has twice

uniformity. For resonator amplitude responses uniform to ± 1 dB, the total spread of resonator frequencies needs to be less than 6 ppm for $Q = 4 \times 10^4$. This requires, for example, that the length of the striplines be uniform to $\approx 0.2 \mu\text{m}$ out of a total length of ≈ 3 cm. While challenging, this goal appeared achievable, since lithographic reproduction is capable of that degree of precision. Indeed, this was one reason for initially choosing to use stripline resonators rather than lumped capacitors and inductors. The problem for the striplines turns out to be the demanding tolerances for the package. This package is the same as that used for the convolver delay lines and the passive chirp filters and requires the use of a second ground plane on a second substrate which is mechanically pressed against the conductor on the primary substrate. Any variations in the gap between the two gives variations in the effective dielectric constant and thus in the propagation velocity and resonant frequency. The existence of any variations in an air gap as large as $.0003 \mu\text{m}$ averaged over a resonator would effectively detune the resonators. Resonator structures were thermally cycled between room and helium temperatures to look for cycle-to-cycle variations of the resonant frequencies. These were determined to be on the order of 1 part in 10^3 . While this is not the same as a measurement of resonator uniformity, we expect that these cycling variations would also result in comparable variations between resonators. It is unlikely that the 3 orders of magnitude improvement necessary can be achieved without radical package redesign.

Faced with this dilemma, we proceeded to look for alternatives and have decided to pursue lower-frequency, lower-Q resonators using lumped capacitors and inductors, but with the same overall integration time. Key issues which needed to be reassessed included circuit area, signal strength, and signal-processing considerations such as bandwidth, dynamic range, and implementation

The magnitude of the integrated ac current will depend on the output level from the mixers at the resonant frequency, the coupling strength between the mixers and the resonators, and the Q of the resonator. However, if the coupling is too strong, the resonator Q will be degraded because of loading from the mixer output circuit. If the effective output impedance of the mixer is equal to the stripline impedance of the resonator, the optimal coupling is found to be $\approx Q^{1/2}$, and the maximum integrated signal is found to be $\approx Q^{1/2}$ times the mixer output. For example, with a Q of 10^5 , the coupling efficiency would be $\approx 0.3\%$, and the integrated signal would be ≈ 300 times the mixer output level. Thus for an output level of $\approx 3 \mu\text{A}$ from the mixers (estimated from the convolver results), a signal level of $\approx 1 \text{ mA}$ is possible. This level compares very favorably to the level required from considering switching noise in the junctions.

Mutual isolation between resonators is required to prevent a signal in one channel from adding to or subtracting from signals in other channels. This problem was especially worrisome, because of the very high Q's of the resonators, because the desired coupling to the resonators from the mixers was already very weak, and because of the inability to contact the ground plane directly through the $125\text{-}\mu\text{m}$ thick substrates. Particular attenuation was paid to potential coupling through the biasing lines for the peak detectors. Floating peak detectors were designed. These were to be situated at the center of a $\lambda_0/2$ resonator, near virtual ground, and to be biased in a symmetrical balanced manner to minimize mutual coupling. This design appears to have adequate isolation levels.

However, the ultimate difficulty with the use of high-Q stripline resonators turned out to be the anticipated inability to achieve adequate

Turning our attention to the requirements for signal processing, we note that these applications do not, in general, require very low error rates but rather demand extreme speed for highly structured data flow. Stringent environmental requirements must also be met. Superconductive technology today can clearly supply the speed and reliability with niobium-based designs. Environmental considerations, such as space and power requirements, depend more on the development of an adequate cryocooler technology than on the device technology itself.

The most frequently encountered function in radar and communications is matched filtering. It is instructive to consider the digital fast Fourier transform algorithm (FFT) as a means to achieve programmable matched filtering. It is possible to quantify the magnitude of the process in terms of the number of arithmetic operations per second (ops). Digital signal processing techniques are highly developed and considerable savings can be realized by employing FFT techniques. But the required computation rate for programmable matched filtering (8) is still at least $20 B \log_2 TB$. Dedicated digital processors can currently provide computation rates of about 2×10^9 ops. Based on this rate, the current bandwidth limits for digital signal processing systems were sized as a function of processing gain and plotted as shown in Fig. 4.

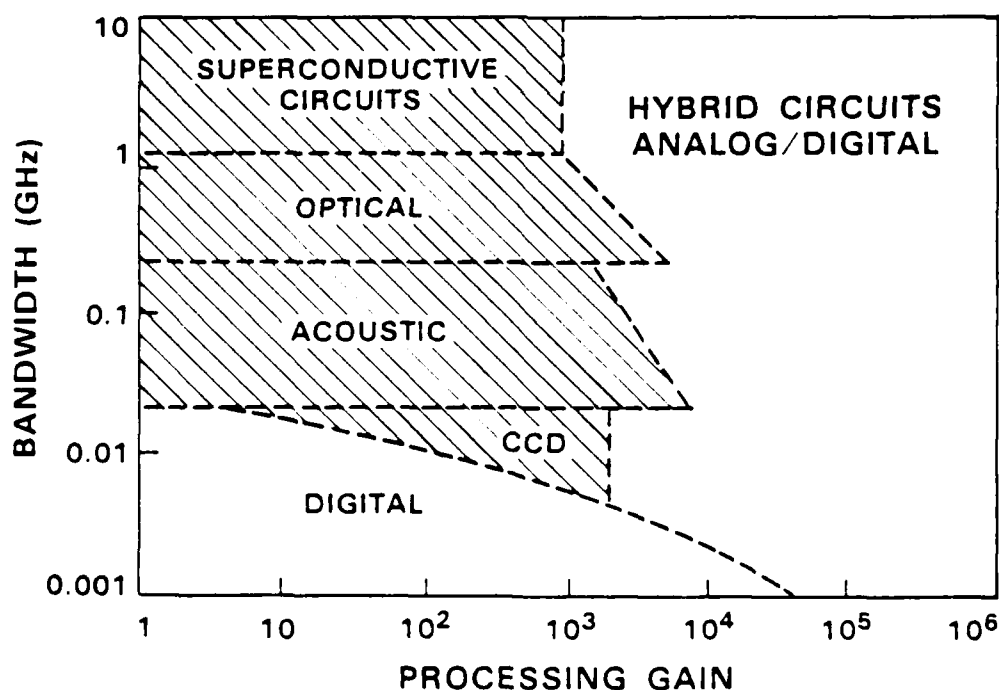


Fig. 4 Projected bandwidth versus processing gain regimes of analog, digital and hybrid signal-processing systems.

Note that in order for signal processing bandwidths to increase by an order of magnitude, computation rates must increase at least as fast. This places a very real limit on the bandwidth capability of

digital signal processors. Conversely, processing gain, dynamic range and accuracy can often be more easily extended in a digital system than in an analog signal processor.

What is the potential for increasing the digital computation rate in the coming decade? In spite of very high speed logic (< 40 ps), the projected computation rate for the Josephson general purpose computer was less than 10^9 ops. This is in large part because the computation rate tends to be limited by propagation delays, clock skews and reset times rather than by the logic switching speeds in both room-temperature and cryogenic systems. Parallel processing systems allow the designer to substantially increase the computation rate. This technique is commonly implemented in dedicated semiconductor processors but at a considerable cost in terms of power and space requirements. Because of the extremely low power requirements (≈ 2 μ W/gate) of superconductive logic, specialized superconductive systems such as array processors could be achieved with extremely dense gate configurations and considerably higher computation rates.

1.4 HYBRID SIGNAL PROCESSING

Many applications, such as signal analysis and matched filtering, require very large signal processing bandwidths. Because of the bandwidth limitations of digital processors, these needs, currently and well into the future, will only be met by analog signal processing devices.

However, in a hybrid (analog/digital) system, an analog device could provide the capability of large processing bandwidth, while digital circuits would extend the available processing gain. Such an implementation has recently been demonstrated with acoustic convolvers (9). Here the convolver preprocessed a 100-MHz waveform, while a binary integrator extended the processing gain.

It is interesting to note that superconductive technology can provide all the elemental analog functions required for signal processing, and all the digital functions as well. This one technology, unlike any other, is therefore fully capable of implementing entire hybrid signal processing architectures. The extended signal processing capability which may be provided by future hybrid systems (superconductive and multiple technology configurations) is also indicated in Fig. 4.

1.5 DISCUSSION

The digital superconductive research activities which were recently curtailed in North America were directed toward the development of high-speed logic and memory circuits for high-performance mainframe computer applications. While the potential market volume is large, it may not have been the most suitable choice for existing cryogenic technology. It is common to judge a new technology in terms of its potential to replace a well-developed technology in existing applications. This seldom happens, even if considerable effort and financial resources are expended on developing the new technology. Rather, the new technology usually finds its market niche in rapidly developing new applications.

Exciting new opportunities exist for cryogenic devices in signal processing applications. Superconductive devices for pulse compression and convolution have recently been demonstrated and are

being further developed. These analog devices offer bandwidth capabilities which are unreachable with other technologies. Yet in applications such as signal sorting and image processing, a real need exists for extremely large bandwidths. Digital circuits fabricated with the same technology can provide very high speed circuits for sampling and data sorting. Hybrid systems implemented with cryogenic circuits may offer the user unparalleled capabilities in signal processing in the future.

1.6 ACKNOWLEDGMENTS

The author gratefully acknowledges R. S. Withers and A. C. Anderson for use of their results on the tapped-delay-line structures and for their collaboration in developing fabrication techniques, and R. W. Ralston and J. H. Cafarella for their advice and guidance.

REFERENCES

1. Reible, S. A., 1982, "Wideband Analog Signal Processing with Superconductive Circuits," 1982 Ultrasonics Symp. Proc., 63-74.
2. Williamson, R. C., 1977, "Measurement of the Propagation Characteristics of Surface and Bulk Waves in LiNbO_3 ," 1977 Ultrasonics Symp. Proc., 323-327.
3. Withers, R. S., Anderson, A. C., Wright, P. V., and Reible, S. A., 1983, "Superconductive Tapped Delay Lines for Microwave Analog Signal Processing," IEEE Trans. Magn., MAG-19, 480-484.
4. Reible, S. A., 1983 "Superconductive Convolver," IEEE Trans. Magn., MAG-19, 475-480.
5. Dhong, S. H., Jewett, R. E. and Van Duzer, T., 1983, "Josephson Analog-to-Digital Converter Using Self-Gating-AND Circuits as Comparators," IEEE Trans. Magn., MAG-19, 1282-1285.
6. Hamilton, C. A. and Lloyd, F. L., 1981, "Design Limitations for Superconducting A/D Converters," IEEE Trans. Magn., MAG-17, 3419-3419.
7. Anacker, W., 1980, "Josephson Computer Technology: An IBM Research Project," IBM J. Res. Develop., 24, 107-112.
8. Cafarella, J. H., 1983, "Wideband Signal Processing for Communications and Radar," Proc. Nat. Telesystems Conf., 55-58.
9. Baker, R. P. and Cafarella, J. H., 1980, "Hybrid Convolver/Binary Signal Processor Achieves High Processing Gain," 1980 Ultrasonics Symp. Proc., 5-9.

Appendix B

Superconductive Delay-Line Technology
and Applications

Presented at the 1984 Applied Superconductivity
Conference, San Diego

"Presented at the 1984 Applied Superconductivity Conference, San Diego. Proceedings to be published in IEEE Trans. Magnetics, 1985."

SUPERCONDUCTIVE DELAY-LINE TECHNOLOGY AND APPLICATIONS*

R. S. Withers, A. C. Anderson, J. B. Green, and S. A. Reible

Lincoln Laboratory
Massachusetts Institute of Technology
Lexington, MA 02173-0073

Abstract

Microwave analog signal-processing filters have been realized in the form of coupled niobium striplines on silicon dielectric substrates. Device responses with ± 2 -dB amplitude accuracy and 9°-rms phase error have been achieved in amplitude-weighted filters with 37.5 ns of dispersion and 2.3-GHz bandwidths. Relative side-lobe levels of -26 dB and less are currently obtained.

The achievable dispersion for stripline circuits on a single pair of 5-cm-diameter, 125- μ m-thick wafers is limited to about 40 ns by the electromagnetic coupling between neighboring lines. To achieve greater dispersion two approaches are under development:

(1) Stripline circuits are being fabricated on multiple wafer pairs which are physically stacked and electrically concatenated to produce dispersive delay lines with 4-GHz bandwidth and 75-ns dispersion time. Phenolic resin is used as an adhesive to ensure the mechanical integrity of the stacked structure. (2) A technique to fabricate dense stripline circuits on very thin (15- μ m) single-crystal silicon superstrates supported by thicker substrates has been demonstrated and preliminary results will be described.

A chirp-transform system capable of real-time spectral analysis has been constructed using a pair of the superconductive delay-line filters. A resolution of 43 MHz over an unprecedented 2400-MHz bandwidth with amplitude uniformity of ± 1 dB and side-lobe levels of -18 dB was demonstrated.

Introduction

Transversal or finite-impulse-response filters are realized in the form of tapped delay lines and are widely employed in wideband analog signal processing applications. Specifically, linear frequency-modulated filters, also known as chirp filters, are valuable components in high-performance radar¹, spread-spectrum communications², and spectral analysis systems³. Critical performance parameters are the dispersion time T , the bandwidth B , and the amplitude and phase deviations from ideal which, in matched-filtering applications, are manifested by degraded side-lobe performance.² Suppression of side lobes to a -40-dB relative level is a common goal and requires, regardless of the technology used to realize the filter, inclusion of amplitude weighting and tight control of both the amplitude- and phase-vs-frequency characteristics of the filter.

*This work was sponsored by the Department of the Army and the Defense Advanced Research Projects Agency.

A technology must offer three essential functions if a transversal filter is to be realized: signal delay, tapping of the signal stream at specified delays and with specified weights, and summation of the tapped signals. Acoustic delay media have been successfully exploited during the last decade to produce high-performance surface-acoustic-wave devices⁴ with bandwidths of several hundred megahertz. Electromagnetic delay media, on the other hand, offer even greater bandwidth (up to a few tens of gigahertz) but the high electromagnetic propagation velocity makes difficult the attainment of large delays. To achieve reasonable delays (10-1000 ns) in a small volume, the transmission lines must be reduced in size. This results in an increased transmission loss and precludes the use of normal conductors. We have exploited the low loss of superconductive transmission lines⁵ to realize transversal filters as miniature tapped electromagnetic delay lines.

Techniques for the design, modeling, fabrication, and packaging of this family of devices have been presented.^{6,7} At that time, operation of devices with 35-ns dispersion and 2.6-GHz bandwidth (already surpassing the nominal goal of 2-GHz bandwidth) was demonstrated. For this family of devices wide bandwidth is easily obtainable whereas dispersion, because of the high electromagnetic velocity and the need to maintain isolation, is dear. Forty nanoseconds is the approximate limit to the dispersion attainable on a single pair of easily handled wafers produced by conventional lapping and polishing techniques. We have built a "baseline technology" around devices of this type, using them as a testbed for relatively rapid testing of design concepts and fabrication techniques. The development of techniques to fabricate and package long-line devices which meet the nominal goal of 500-ns dispersion is proceeding concurrently.

In this paper are presented the recent developments of our baseline technology which include: (1) the application of various filter weighting functions including a new partitioning of amplitude-weighting functions which permits exploitation of the phase-conjugate property of the superconductive devices and the consequent use of a filter as its own matched filter; (2) the fabrication of wide, low-impedance lines which require less critical control of linewidth; and (3) the establishment of controls needed to ensure side-lobe suppression and device reproducibility. Two techniques for achieving longer delay will be presented: (1) The electrical cascading of multiple wafer pairs produced by the baseline techniques; and (2) the fabrication of delay lines on very thin dielectric wafers bonded to thicker support wafers. Finally, the use of baseline-technology devices to perform real-time spectral analysis over a 2400-MHz bandwidth is presented.

Baseline Technology

Function of the Baseline Technology

The purpose of the baseline technology is to provide a rapid turn-around test vehicle to identify and eliminate sources of irreproducibility, establish and/or extend the limits of device performance, and test new designs without waiting for the development of long-delay-line techniques. Lines fabricated on 5-cm-diameter, 125- μ m-thick silicon wafers provide that test vehicle. The lessons learned with baseline devices are expected to be applicable, with appropriate scaling, to long-line devices.

Device Structure

The basic device cross section is shown in Fig. 1 and was discussed previously⁶. A coupled pair of superconductive striplines of width w is separated by a variable distance s . The striplines are surrounded by two layers of low-loss dielectric of thickness h which are coated with superconductive ground planes.

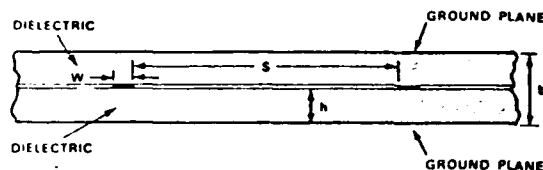


Fig. 1. Cross section of the coupled stripline structure.

The two lines are coupled by a cascaded array of backward-wave couplers as shown in the schematic of Fig. 2. Each coupler has a peak response at frequencies for which it is an odd number of quarter-wavelengths long.⁸ If the length of the couplers is proportional to the reciprocal of distance down the line, then the resulting structure has a local resonant frequency which is a linear function of delay. In other words, it is a chirp filter with a linear group-delay-vs-frequency (or quadratic phase) relationship. The strength of each coupler is controlled by varying the line spacing s to give a desired amplitude weighting to the response.

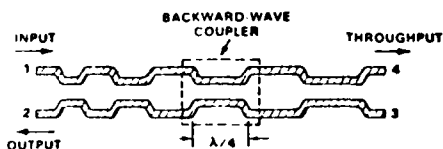


Fig. 2. Chirp filter formed by cascading backward-wave couplers between adjacent electro-magnetic delay lines.

Design and Analysis

The design and analysis of stripline tapped-delay-line chirp filters was described previously.⁶ The designer specifies the desired center frequency, bandwidth, insertion loss at center frequency, and weighting function. A grating function (coupling vs spatial coordinate) is generated which includes a correction for amplitude

distortions caused by strong coupling and the consequent input wave depletion. The design is analyzed using a coupling-of-modes solution; predistortions of the grating phase can be introduced at this point to compensate for phase distortions caused by strong coupling⁹ and the procedure iterated. From the grating function an electromagnetic analysis is used to specify the line spacing function, and a photomask is generated.

In typical systems employing chirp filters, one filter has a flat amplitude response, the full amplitude weighting function being carried by the second (quasi-matched) filter. Unlike most chirp filters, however, the superconductive tapped delay lines are four-port devices and, provided that propagation losses are small and the grating coupling is not too strong, the coupled responses (S_{12} and S_{34} in Fig 2) are phase-conjugate; that is, the impulse response from one end is the time-reverse of that from the other. One filter can thus serve as its own matched filter. By weighting the filter with the square root of the desired weighting function, the overall response of a pulse-compression system will be the desired one. In some applications (e.g., spectrum analysis), however, this partitioning of weighting functions is disadvantageous and separate flat and fully weighted filters must be used.

Filters with characteristic impedances less than 50 ohms offer several advantages: (1) the greater width of the lines (for example, on silicon 25-ohm lines are four and one-half times the width of 50-ohm lines) reduces the sensitivity of the impedance to linewidth variations, thereby reducing spurious reflections; (2) conductor losses become asymptotically smaller as the parallel-plate limit is approached; and (3) the perturbation in effective dielectric constant caused by voids between the dielectric layers are minimized in the parallel-plate limit. The first point is especially important as we scale down linewidths for thinner substrates. There is, however, some increase in sensitivity of impedance to substrate thickness.

Provision for impedances other than 50 ohms is included in the design routines. Integral tapered-line transformers¹⁰ which present 50-ohm impedances at the device ports are included. Devices with 25-ohm lines have been fabricated; results are presented in a following section.

Fabrication & Packaging

The delay line shown schematically in Fig. 2 would be difficult to fabricate, being typically 1-mm wide and 3-m long. To utilize round substrates with a minimum number of small-radius bends, the delay line is wound up into a quadruple-spiral configuration, with all four electrical ports brought to the wafer edge.

The lower wafer (cf. Fig. 1) carries a niobium ground plane on its lower surface and the niobium stripline pattern on the upper surface. The upper wafer carries a single niobium ground plane.

The niobium films are deposited to a thickness of 3000 Å by RF sputtering and patterned by reactive ion etching.¹¹ The two substrates are 5-cm-diameter, 125- μ m-thick silicon wafers. The use of high-resistivity silicon as a low-loss dielectric substrate has been discussed.⁷ Recent resonator measurements indicate that wafers with resistivities as low as 3 ohm-cm can support TB products of 1000.

In the package,⁷ the second wafer with its ground plane is held in place against the patterned wafer by an array of springs, preventing air gaps which would cause spurious electrical responses. The four RF terminals, brought to bonding pads at the wafer edge, are connected with multiple short wire bonds to SMA connectors brought through the back of the package. Although other laboratories use the wedge bonding of aluminum wires directly to niobium, we find it convenient to evaporate Ti/Au (200 Å/5000 Å) films on top of the niobium pads, to which gold wires can be ball-bonded. These connections are reliable, can be removed for wafer cleaning, repackaging, or other processing without destroying the underlying metallization, and, provided that residual niobium oxides are stripped by a brief dilute HF dip prior to Ti/Au deposition, exhibit little resistance (0.2 ohm). The Ti/Au layer, patterned by liftoff of a spot-exposed photoresist layer, is also utilized to repair defects in the Nb striplines.

Electrical Performance

Fig. 3(a) shows the measured and predicted magnitudes of the frequency response of a flat-weighted filter and Fig. 3(b) shows those of a Hamming-weighted filter. Each device was designed to

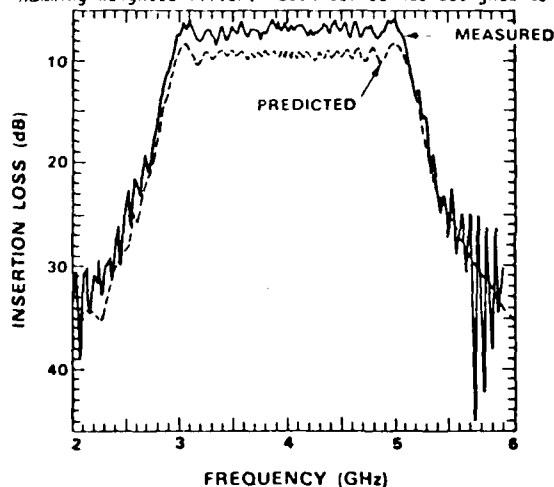


Fig. 3. (a) Predicted and measured insertion loss of a flat-weighted filter.

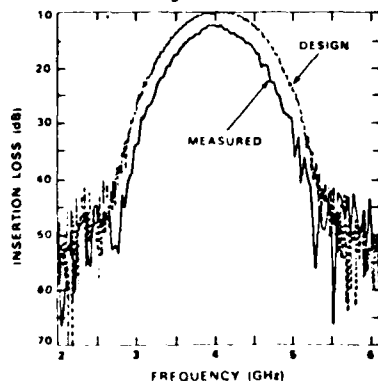


Fig. 3. (b) Insertion loss of a Hamming-weighted filter.

have a 4-GHz center frequency, 2.32-GHz bandwidth, 37.5-ns dispersion, and 10-dB insertion loss.

The 1.5-dB loss of the coaxial dewar probe has not been subtracted from the measured device responses and accounts for much of the error in the Hamming-weighted device. In the case of the flat-weighted device, an error in assembly was found to have resulted in the use of a 210- μ m-thick upper wafer instead of the design value of 125 μ m. Modified to include this deviation from design, the coupled-mode theory predicts a grating insertion loss of 5.5 dB which, after inclusion of the probe loss, is in close agreement with the measurement.

The phase of a linear chirp filter is designed to be a quadratic function of frequency, the quadratic coefficient being proportional to the "chirp slope" of the device $1/B$. A least-squares fit to the measured phase data of the flat- and Hamming-weighted devices of Fig. 3 revealed chirp slopes of 0.4% and 1.0%, respectively, below the design value, and rms deviations from quadratic of 11° across the full device bandwidth and 9° across the central 2 GHz of bandwidth, respectively.

The fidelity of the phase and amplitude characteristics of these filters is borne out in pulse-compression performance, obtained both in time-domain measurements and by multiplication and transformation of the frequency-domain data. Relative side-lobe levels of -26 dB were obtained when using the flat- and Hamming-weighted devices as matched filters, and -32-dB levels were obtained when the latter device was used as its own matched filter. Devices free of phase and amplitude errors would produce -41-dB side lobes.

Devices have been weighted with the square root of the Hamming function to give an overall Hamming response when using a single line as both expander and compressor in pulse-compression tests. Side-lobe levels of -28 dB and phase deviations of 3.4° rms across the central 1.5 GHz of bandwidth have been obtained.

Tapped delay lines with 25-ohm characteristic impedance were made by using 173- μ m-wide lines on 125- μ m silicon. Tapered transformers¹⁰ of 1-ns length were incorporated to bring the impedance to 50 ohms at all four ports. The available dispersion on 5-cm-diameter wafers was reduced to 27 ns by the wider lines and the transformers. A 25.8-ohm impedance was measured by time-domain reflectometry and a VSWR of less than 1.5 was observed. The 2.6-GHz-bandwidth root-Hamming-weighted devices exhibited a 7° rms phase error over the central 2 GHz of bandwidth and -27-dB side lobes.

Impact of Fabrication on Performance

Two fabrication-related issues have been shown to exert a particularly strong effect on device performance:

(1) Wafer thickness variations. The strength of 30-dB backward-wave stripline couplers varies by approximately 1 dB for every 8% change in substrate thickness of either wafer, and 60-dB couplers experience a 1-dB coupling variation for every 4% change in thickness. A uniform error in thickness, as in the device of Fig. 3(a), causes a nearly frequency-independent error in insertion loss. Thickness errors which are nonuniform across the wafer surface, however, cause frequency-dependent amplitude errors and serious side-lobe degradation. A Hamming-weighted filter on a wedge-shaped substrate

with a total thickness variation equal to 10% of its thickness was predicted, using a modified coupling-of-modes analysis, to have a 31-dB relative side-lobe level. To first order, thickness variations do not cause phase errors, as the effective dielectric constant and hence phase velocity are not affected.

(2) Gaps between wafers: The presence of gaps between the two dielectric wafers lowers the effective dielectric constant of the structure and consequently increases the propagation velocity. Phase distortions result. Even if the gap is uniform over the wafer area, the inhomogeneous dielectric also produces differences in even- and odd-mode velocities and thus forward coupling and consequent amplitude errors. Gaps can result from several imperfections: (1) failure of the package to provide sufficient pressure to clamp the two wafers (8.8×10^4 N/m² is currently used); (2) the unavoidable step caused by the niobium thickness, possibly made larger by the nonselectivity of the RIE process and consequent etching of the silicon itself following the removal of the niobium; and (3) nonplanar wafer surfaces.

The presence of gaps can be monitored by measurement of the chirp slope from which is inferred the effective dielectric constant. Numerous devices were tested which revealed effective constants as low as 10.0 instead of the design value of 11.4; poor overall performance was also noted. Investigation led to the conclusion that the third factor listed above was the cause. Single-side-polished wafers had been used as substrates. The spiral pattern was always defined on the polished surface and the deposition of the ground plane on the rough backside appeared to cause no degradation. However, the upper ground plane was deposited on the polished surface, requiring that the bare rough surface be assembled in contact with the spiral Nb pattern. These commercially etched surfaces were found to have an rms roughness of as much as 6000 Å on lateral scales of 20 to 100 µm, in comparison with polished surfaces with rms roughnesses of 50 Å. The rms gap could easily exceed twice the roughness because of the peaked nature of the surface. Even in the parallel-plate limit, such a 0.5% void fraction (based on 125-µm-thick wafers) would, with a high-dielectric-constant material such as silicon, result in a 6% decrease in effective dielectric constant. With the simple corrective measure of using polished mating surfaces, effective dielectric constants of 11.5 ± 0.1 are achieved uniformly.

Long Delay Lines

Requirements

Bandwidths of several gigahertz are relatively easy to achieve with electromagnetic delay lines. Dispersion, however, is difficult to obtain because of the high propagation velocities.

The conductor loss of superconductive stripline increases with frequency and varies as the reciprocal of substrate thickness. Based on the assumption that the maximum tolerable attenuation of a dispersive delay line is 3 dB, the limit imposed by loss on the length of a niobium delay line operating at 4.2 K with a 4-GHz center frequency and 2.7-GHz bandwidth is about 13 µs on 125-µm-thick silicon and 1.0 µs on a 10-µm-thick substrate. Devices with these frequency specifications and a 370-ns dispersion (TB=1000) require, assuming 55-dB isolation, areas of 200 cm² and 16 cm², respectively, on these two

substrates. It is apparent that, to reach the nominal goal of TB=1000, one must either: (1) use large-area (>100 cm²) 125-µm-thick substrates; (2) electrically cascade filter sections on multiple 5-cm-diameter, 125-µm-thick ("baseline") substrates; or (3) use thinner 5-cm-diameter substrates. The first option is not under aggressive development because of the difficulty in handling large, thin wafers. The other two are being pursued in parallel.

Stacked Substrates

Two additional problems are encountered in cascading baseline-technology wafers: (1) physically holding them together in the package and (2) making the necessary rf connections from wafer to wafer. A packaging scheme which addresses these aspects is shown in Fig. 4.

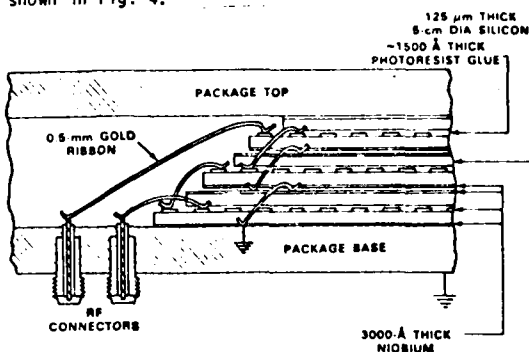


Fig. 4. Stack of three stripline wafer pairs. The connections to the ground planes and one of the two coupled lines are shown.

Two or more stripline assemblies (4 or more wafers) can in principle be held together by spring pressure in the same package used to house single assemblies. However, the possibility of relative motion during assembly makes the electrical bonding operations difficult. For this reason, phenolic resin (AZ 1350B photoresist) is used as an adhesive between each wafer pair to ensure the mechanical stability of the stacked structure. Measurements on a Nb-on-Si resin-bonded resonator demonstrate that a 375-nm film at the stripline interface increases the effective loss tangent of the 250-µm-thick structure by less than 2×10^{-5} . To ensure reliable, uniform contact, both mating surfaces must be polished and coated with resin. The resin losses do not impose severe limits on devices on 125-µm-thick substrates but could limit attainable TB products on thinner substrates.

The resonator measurements also demonstrated a repeatability of resonant frequencies of approximately one part in 10,000 after each of five thermal cycles between room and liquid-helium temperatures. This stability is a factor of six better than that of the same device using the identical spring-loaded package without resin. The technique therefore offers improvement for single-wafer-pair devices as well.

As suggested by Fig. 4, which for simplicity shows only half of the connections needed for a proximity-tapped delay line, low-parasitic-inductance interconnections are made with short ribbon or multiple-wire bonds. Distances are kept short by placing the bonding pads of one wafer nearly on top of the mating pads on the wafer below and slightly

displacing the upper wafer laterally. Time-domain reflectometry indicates that the interlayer parasitic elements are comparable to those of the coax-to-stripline connections.

The interlayer connection may be viewed as a vertical cut across the schematic in Fig. 2. The cut is designed to occur in the "uncoupled" section between neighboring couplers, but unavoidably the round-trip connection length used in practice exceeds the one-half wavelength allowed in design. To avoid a phase discontinuity, an integral number of wavelengths must be added to the allowed half-wavelength round-trip coupled-section-to-coupled-section distance. To avoid a jump in group delay, this length is not merely inserted into the tapped delay line; rather, coupling sections are omitted, one for each extra wavelength. This results in a slight increase in the insertion loss at the local resonant frequency at the transition, but this can to first order be compensated by increasing the strength of the neighboring couplers.

The compressed-pulse response of a 2.6-GHz-bandwidth, 75-ns-dispersion, root-Hamming-weighted filter fabricated on two pairs of 125- μ m-thick silicon wafers is shown in Fig. 5. Its transition length is not an odd number of half-wavelengths, and the -16-dB side lobes result. A corrected design is in fabrication.

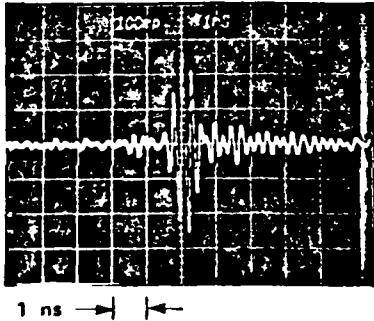


Fig. 5. Compressed-pulse response of a two-wafer-pair chirp filter. The device has a 2.6-GHz bandwidth, 75-ns dispersion, and root-Hamming weighting.

Thin Supported Wafers

Techniques for the fabrication of very thin dielectric superstrates supported by thick substrates with an intervening superconducting ground plane were discussed previously. These techniques have been refined and usable assemblies are now being produced.

The steps in the process may be envisioned with the aid of Fig. 6 and are: (1) growth of a high-resistivity layer of epitaxial silicon on a heavily doped n-type Si wafer; (2) RF-sputter deposition of a Nb film onto the epitaxial layer; (3) bonding of the Si wafer to a 7740 glass (Pyrex) wafer using a low-temperature electrostatic bonding technique, with the Nb at the interface of the two wafers; (4) removal of the heavily doped silicon by a combination of mechanical lapping, nonselective and resistivity-selective chemical etching; (5) removal of a small area of the exposed epitaxial layer to allow contact to the interfacial Nb layer which will serve as the ground plane of the device that will be built on the epilayer; and (6) deposition of a Nb

thin film on the silicon which can later be photolithographically patterned to form the stripline central conductor.

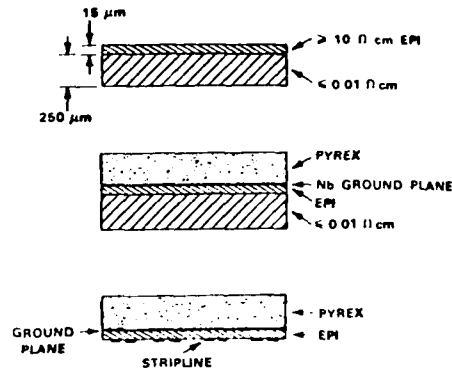


Fig. 6. Fabrication of 15- μ m-thick silicon wafers by epitaxial growth, electrostatic bonding, and preferential etching. Top: starting epitaxial wafer. Middle: assembly after deposition of Nb ground plane and bonding to support wafer. Bottom: completed structure after preferential removal of substrate, niobium deposition, and patterning of the stripline.

Fig. 7 is a photograph of a wafer which has completed the first four steps of the process. The four defects are small holes which were caused by particulates at the Nb/Pyrex interface. The particulates caused local deformations which were etched through by the selective etch. The contamination has since been eliminated and defect-free layers are produced. The finished silicon superstrate has a thickness uniform to less than 1 μ m, comparable to the uniformity of the original epilayer.

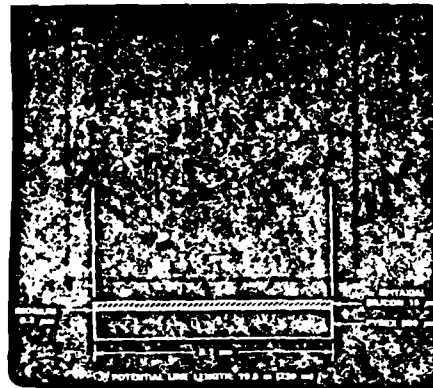


Fig. 7. 15- μ m-thick epilayer bonded to Pyrex with intervening niobium film.

To our knowledge this is the first electrostatic bonding¹² of a niobium film to glass. To ensure uniform bonding, care must be taken that there is no epilayer "crowding" at the wafer edge. The possibility that a niobium/glass reaction may occur at the 400°C bonding temperature and adversely affect

the superconducting properties of the opposite (silicon) side of the film is being investigated by resonator measurements. The bonded Si/Nb/glass assemblies have been cycled to 4.2 K and exhibited no deleterious effects.

The resistivity-selective etch¹³ used to remove the heavily doped substrate is an HF: HNO₃: acetic mixture. Under optimum conditions the etch is very selective but it is inherently unstable; the generation of HNO₃ degrades the selectivity and necessitates careful monitoring. Potassium hydroxide has been used to etch holes through the epilayer without attacking the underlying niobium, permitting establishment of contact to the ground plane.

Resonator measurements are being conducted to ensure that recombination centers in the epitaxial silicon do not contribute to hopping conduction and increase the dielectric loss. A 25-ohm, 220-ns-long delay line will be built on the 15- μ m superstrates. Delays of up to 500 ns with a 5-dB loss at 5 GHz are expected to be achievable on a 5-cm-diameter, 9- μ m-thick superstrate.

Spectrum Analysis

Configuration

An important application of chirp filters is the real-time spectral analysis of wideband signals. Flat- and Hamming-weighted filters have been used as dispersive elements in a chirp-transform³ real-time spectrum analyzer.

The configuration shown in Figure 8 is used. This arrangement is termed the multiply-convolve arrangement³ because of the multiplication of the input signal by a chirp waveform followed by convolution of the product with a chirp waveform in the compressor.

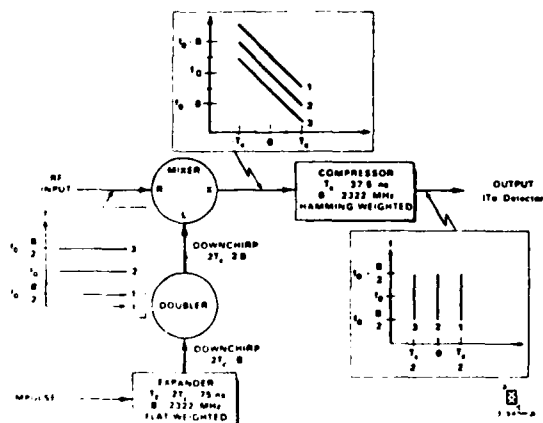


Fig. 8. Chirp-transform spectrum analyzer employing superconductive expander and compressor. Frequency-time plots are shown for various points in the signal path. The RF signal input shown in the figure is an example of the possible signals within the $f_0 - B/2$ to $f_0 + B/2$ analyzer input band; in this case three tones are shown, one at f_0 , a second at $f_0 - B/2$, and a third at $f_0 + B/2$. These are mapped by the analyzer into time slots spaced by $T_c/2$.

The mixer used to form the product of the chirp and the RF input is a commercially available unit with broadband IF characteristics. All components, including amplifiers and filters not shown in Figure 8, operate at room temperature except for the expander and compressor, which operate in liquid helium at 4.2 K.

Performance

Figure 9 shows the compressor output in response to seven sequential CW tones from 3400 to 4000 MHz in 100-MHz increments. The system responds to RF inputs from 2.8 to 5.2 GHz with an amplitude uniformity of ± 1.2 dB. From Figure 9 the dispersion rate of the analyzer is measured to be 61 MHz/ns, in good agreement with the designed device chirp slope of 61.9 MHz/ns.

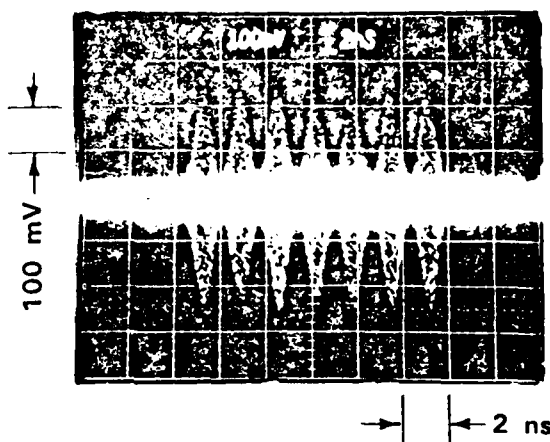


Fig. 9. Multiple exposure of sampling-scope output for successive single-tone inputs of 4000 MHz (leftmost pulse) to 3400 MHz (rightmost pulse) in 100-MHz increments. The input power level is -7 dBm.

The width of the peaks at the -4 dB level is 0.7 ns, implying a two-tone frequency resolution of 43 MHz. For comparison, the expected resolution, which is the inverse of the compressor dispersion multiplied by a factor to account for the broadening caused by the Hamming weighting,¹ is 39.2 MHz.

The compressor output amplitude is a linear function of the RF input amplitude for input power levels up to 3 dBm. Input CW signals of -43 dBm can be resolved from the noise floor set by the thermal noise of the room-temperature electronics, implying a dynamic range over the noise floor of 46 dB.

Side-lobe levels of 18 dB below the peak are observed. The dispersive delay lines themselves, in pulse-compression tests, exhibit -24-dB side lobes; thus, the added degradation is due to distortions in the room-temperature mixers, amplifiers, and filters.

Conclusion

These superconductive devices have, with only a few years of development, surpassed many of the performance goals of competing signal-processing technologies such as optical and magnetostatic technologies. A complete theoretical understanding of these superconductive analog signal processing

devices has been demonstrated. A baseline technology for the reproducible fabrication of wide-bandwidth but modest-dispersion devices has been established. The development of devices with greater dispersion is proceeding on two fronts. Operation of the devices in an important applications area, spectral analysis, has been demonstrated.

Two areas need development before extensive application of this technology will be made. First, circuits must be developed which can acquire the wide-bandwidth output of the delay lines and, in real time, extract the essential information for further processing by room-temperature digital processors. Josephson circuits for this purpose are being developed in several institutions and cooled semiconductor and optoelectronic means are also under consideration. Second, compact cryocoolers capable of bringing these low-power circuits to their operating temperatures are needed. These delay lines, employing a single superconductive layer, are likely candidates for the application of low-RF-loss high- T_c materials which are expected to raise the operational temperature to at least 8 K.

Acknowledgements

The authors wish to thank R. W. Ralston for guidance and support, C. M. Vanaria for fabrication and packaging, S. S. Cupoli for microwave testing, J. A. Marden for thin-silicon bonding and etching, and K. A. Lowe and S. M. Lavache for manuscript preparation.

References

1. C. E. Cook and M. Bernfeld, Radar signals. NY: Academic, 1967.
2. R. W. Ralston, "Signal Processing: Opportunities for Superconductive Circuits," 1984 Applied Superconductivity Conference, San Diego, CA.
3. G. W. Judd and V. H. Estrick, "Applications of SAW chirp filters -- an overview," *Proc. Soc. Photo-Opt. Instrum. Eng.*, vol. 239, pp. 220-235, 1980.
4. R. C. Williamson, "Properties and applications of reflective-array devices," *Proc. IEEE*, vol. 64, no. 5, pp. 702-710, May 1976.
5. R. L. Kautz, "Miniaturization of normal-state and superconducting striplines," *J. Res. Nat. Bur. Stand.*, vol. 84, no. 3, p. 247, May 1979.
6. R. S. Withers, A. C. Anderson, P. V. Wright, and S. A. Reible, "Superconductive tapped delay lines for microwave analog signal processing," *IEEE Trans. Magnetics*, vol. MAG-19, pp. 480-484, 1983.
7. A. C. Anderson, R. S. Withers, S. A. Reible, and R. W. Ralston, "Substrates for superconductive analog signal processing devices," *IEEE Trans. Magn.*, vol. MAG-19, pp. 485-489.
8. B. M. Oliver, "Directional electromagnetic couplers," *Proc. IRE*, vol. 42, no. 11, pp. 1686-1692, Nov. 1954.
9. R. S. Withers and P. V. Wright, "Superconductive tapped delay lines for low-insertion-loss wideband analog signal-processing filters," *Proceedings of the 37th annual symposium on frequency control*. Philadelphia: IEEE, 1983, pp. 91-86.
10. R. W. Klopfenstein, "A transmission-line taper of improved design," *Proc. IRE*, vol. 56, pp. 31-35, 1956.
11. S. A. Reible, "Reactive ion etching in the fabrication of niobium tunnel junctions," *IEEE Trans. Magn.*, vol. MAG-17, no. 1, pp. 303-306, Jan. 1979.
12. G. Wallis, "Field assisted glass sealing," *Electrocomp. Sci. and Tech.*, vol. 7, no. 1, pp. 45-53, 1975.
13. H. Muraoka, T. Ohhashi, and Y. Sumitomo, "Controlled preferential etching technology," in *Semiconductor Silicon 1973*, H. R. Huff and R. R. Burgess, eds. Princeton, NJ: Electrochem Soc., 1973, pp. 327-338.

Appendix C

Superconductive Convolver with Junction Ring Mixers

Presented at the 1984 Applied
Superconductivity Conference, San Diego

SUPERCONDUCTIVE CONVOLVER WITH JUNCTION RING MIXERS*

S. A. Reible⁺

Lincoln Laboratory, Massachusetts Institute of Technology
Lexington, Massachusetts 01730-0073

Abstract

Convolver Operation

A superconductive convolver with tunnel-junction mixers has been developed and demonstrated as a programmable matched filter for near 1-GHz-bandwidth periodic waveforms. A low-loss, 14-ns-long superconductive stripline circuit provides temporary storage relative shifting of signal and reference waveforms. These waveforms are sampled by 25 proximity taps and local multiplication is performed by 25 tunnel ring mixers. Two short transmission lines recently sum the local products and deliver the convolution output. The output power level of the convolver has been increased 18 dB by the incorporation of junction ring mixers and other output circuit improvements. The mixers employ series arrays of niobium/niobium-lead junctions driven by delay-line taps in a balanced manner. The ring mixer provides higher output power levels (to -58 dBm), improved suppression of undesired mixing products and higher rf impedances than the single-junction mixers used in the previous device. Convolver can provide the essential programmable matched-filter component for extremely-bandwidth spectral analysis or spread-spectrum communication systems. The current device has a 2-GHz signal bandwidth and a time-bandwidth (TB) product of 10⁴ produced compressed pulses with -7 dB peak-side-lobe levels. Design improvements to be described include increasing the TB product to 100 and reducing spurious side-lobe levels.

Introduction

The first demonstration of a superconductive convolver was described at the 1982 Applied Superconductivity Conference.¹ This device employed a niobium stripline as a low-loss delay element² and niobium-lead junctions as mixing elements. Because of the low saturation level of the niobium-lead junction mixers, the output level of this device was only marginally greater than the thermal noise level set by wideband room-temperature amplifiers.

Superconductive ring mixers with series arrays of niobium-lead junctions were developed and incorporated in a convolver design. The mixer ring provides higher output power levels and, with a quadrature feed, achieves a nominal 10-dB suppression of undesirable self-products. The delay line and device package were redesigned to incorporate a stripline structure resulting in lower phase distortion and more reliable electrical characteristics. Device operation as a narrow-band programmable matched filter was demonstrated using linearly frequency-modulated (chirped) waveforms.

A convolver can provide the essential signal processing function in communications for wideband spread-spectrum waveforms.^{3,4} The programmable feature of convolvers allows the encoding waveform to be changed from bit-to-bit, thereby providing maximum signal processing flexibility and resistance to repeating and enabling secure communications. Devices with very large bandwidths such as superconductive convolvers can accommodate very high data rates while maintaining covertness.

This work was sponsored by the Air Force Office of Scientific Research.
Present address: MICRILOR, P.O. Box 624, Swampscott, MA 01907

Operation of the superconductive convolver is shown schematically in Fig. 1. A signal $s(t)$ and a reference $r(t)$ are entered into opposite ends of a superconductive delay line. Samples (delayed replicas) of the two counterpropagating signals are taken at discrete points by proximity taps weakly coupled to the delay line. Sampled energy is directed into junction ring mixers which produce mixing products. The mixing products are spatially integrated by summing in multiple nodes connected to one or more short transmission lines. The summed energy which appears at the output port of the device includes the desired cross-product (signal times reference), undesired self-products as well as higher-order terms. Because both of the spatial patterns are moving, there is a halving of the time scale at the output; that is the center frequency and bandwidth are doubled. If the reference is a time-reversed version of a selected waveform, then the convolver functions as a programmable matched filter for that waveform.

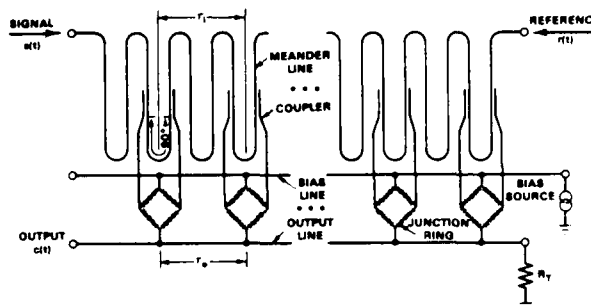


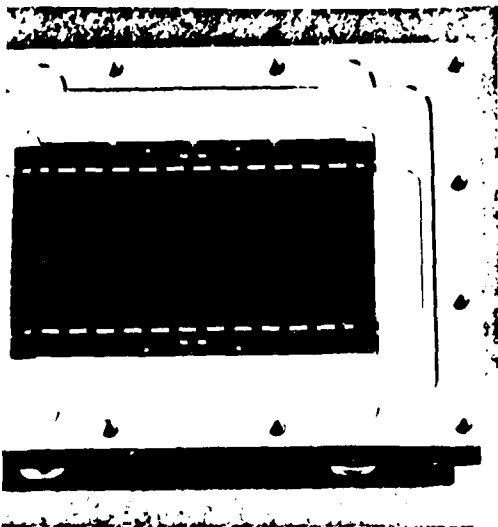
Fig. 1 Schematic of the superconductive convolver.

Convolver Design

Stripline Structure and RF Package

A photograph with an overview of the principal electronic circuitry of an unassembled convolver is shown in Fig. 2. The circuits are fabricated on a 125- μ m-thin, 2.5 x 4 cm² sapphire substrate with a niobium ground plane deposited on the reverse side. The central region of the device consists of a 14-ns meander delay line with a 50-ohm characteristic impedance. Twenty-five proximity tap pairs, located along opposite sides of the delay line, sample the propagating waveforms and direct the sampled energy into a corresponding number of junction-ring mixers. The resultant mixing products are collected and summed by two low-impedance (15 ohm) transmission lines located near opposite edges of the rectangular substrate. Each end of the output transmission line has a tapered line section which transforms the characteristic impedance of the line to a standard 50 ohms. The desired outputs from the two transmission lines are then summed externally with a microwave combiner.

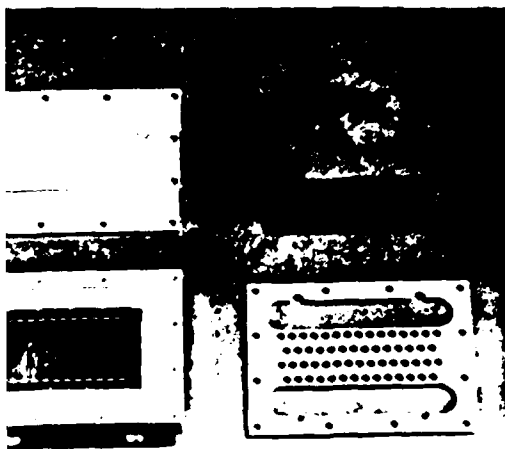
During device assembly a second sapphire substrate with another niobium ground plane (shown in Fig. 3) is placed against the delay line region of the first substrate to form a stripline circuit. Alignment of these two substrates to each other is determined by slots which have been machined in the base package. The top sapphire dielectric/niobium ground plane structure



nine substrate with superconductive
units mounted in base plate.

and the edge of the niobium delay line but
overlap the mixers or output line. A spring
is mounted over the top substrate and 52
upper springs are inserted. A central cover
is added which compresses the springs and
applies 48 newtons of force holds the two sap-
rates in intimate contact. Wire leads are
connected to the device pads and RF connectors for
connection. Finally, two additional cover
is added for mechanical protection.

under delay line design for this device con-
sists of straight-line sections connected by 180-
degree bends. Unfortunately, these bends slightly
change the line impedance and cause reflections. With
high frequencies, the effects of these reflections can be
significant. Weak coupling between adjacent sections of
the line is another potential source of re-
flection. Because the bends are periodically spaced,
reflections add coherently at certain frequencies
creating stop bands in the transmission response of
the line. These stop bands occur at fundamental
resonant frequencies of $(2t_d)^{-1}$ where t_d is the
delay time. The design intentionally places the
pass band (3-5 GHz) between the 1st and 2nd



Photograph of convolutioner substrates and major
package plate parts.

Junction Ring Mixer

The ring mixer has two RF input ports, a single
output port and a dc bias port. Each of its active legs
has several superconductive tunnel junctions in series.
The bias ports are connected to a common current source
while the output ports are connected to one of the two
output lines. Two terminals on opposite sides of each
ring are excited by RF inputs from individual proximity
couplers. The two couplers are separated by a nominal
90 degrees on the input delay line and ideally, except
for a phase shift, carry equal signal (f_1) and
reference (f_2) components to the mixer terminals. The
desired mixing term ($f_1 + f_2$) between the signal and
reference is coherently summed at the lower terminal of
the diode ring and directed into a common output line.
In addition to the desired mixing term, undesired
self-products of the signal ($2f_1$) and reference ($2f_2$)
arrive at the output terminal. But the self-products
from the two arms of the ring arrive at the output
terminal approximately 180 degrees out of phase and
effectively cancel each other. Computer simulation
indicates that this technique has the potential of
providing a 14-dB suppression of this spurious output
over the desired 40% fractional device bandwidth; tests
on individual junction ring mixers indicated a nominal
10 dB suppression. A major limitation at the present
time is that the sampling weight of the taps is
somewhat dependent upon the direction of propagation on
the input delay line. Therefore, both input ports of
the ring mixer do not always receive the same magnitude
of sample of the signal (or reference) waveform.
Another limitation is that the proximity couplers are
not terminated in their characteristic impedance and
that resultant multiple reflections in the couplers can
cause considerable phase distortion.

A photograph of a junction ring mixer is shown in
Fig. 4. The structure has a series array of four tunnel
junction in each of its four legs. The junctions
consist of a niobium base electrode, a niobium oxide
tunnel barrier and a lead counterelectrode.⁵ Junction
areas are defined by 4- μ m-diameter windows etched in a
silicon monoxide insulation layer. Input and output
signals are coupled into and out of the diode rings
through microstrip transmission lines. Stray RF
currents on the bias line are terminated with pad-type
capacitors.

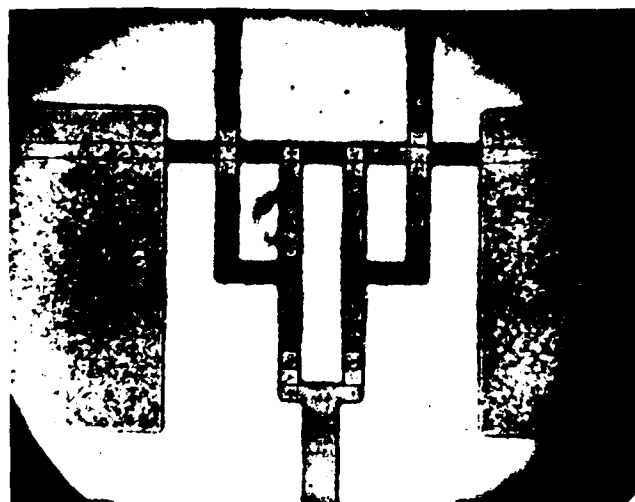


Fig. 4 Photograph of sixteen-junction ring mixer.

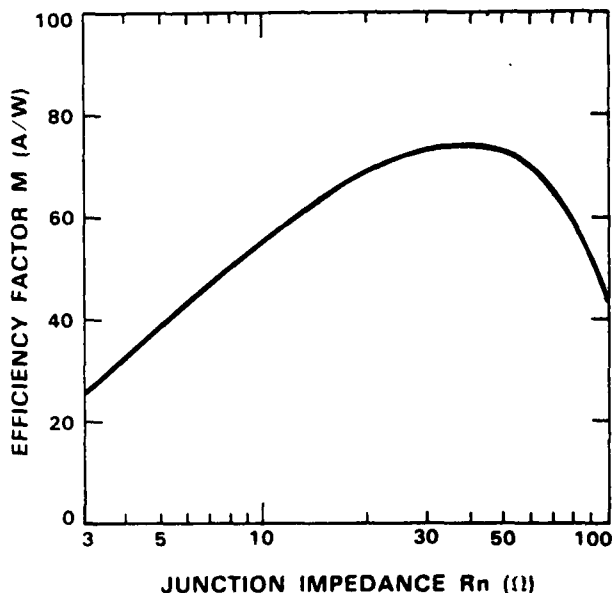


Fig. 5 Predicted efficiency M of ring mixer as a function of normal-state junction resistance (R_n).

To properly design convolvers and to project their performance, it is necessary to have models which predict mixer efficiency and saturation. Nonlinear circuit models which fulfill this function have been developed. The efficiency of the mixing interaction is defined as

$$M = I_T / (P_r P_s)^{1/2},$$

where P_r and P_s are the input powers diverted into the mixer network and I_T is the output current into the load. A plot of the predicted values for M in a convolver structure is shown in Fig. 5. Both M and loading of the output circuit by the ring mixers is strongly dependent upon junction impedance.

Output Circuit

To achieve a properly functioning device, the desired product from each mixer must add in phase at the the output port of the device. Because the collection nodes along the output transmission line are separated by finite delay, excessive phase distortion can result in the superconductive convolver. This phase distortion has been compensated to first order in acoustoelectric convolvers by offsetting the center frequency of the reference relative to the center frequency of the signal.⁶ This technique is currently employed in the superconductive convolvers. Half of the available output power propagates towards each of the ports at opposite ends of the output line. Since the output phase distortion can only be compensated for one direction of signal propagation, one port of each output line is selected for summation and the second port is terminated in its characteristic impedance. Other frequency terms such as the undesired self-products have a different phase-vs-position relationship and hence usually do not add coherently at the output.

Device Measurements

To determine device characteristics, the convolver was first evaluated with CW input tones. The real-time output of the convolver with CW input tones gated to a

14-ns duration and entered into signal and reference ports is shown in Fig. 6(a). The envelope of the convolver output has a triangular shape as predicted for the convolution of two nearly square (1-ns risetime) input envelopes. The trailing side-lobes are associated with reflections in the measurement set and spurious signals in the device. The convolvers have a measured efficiency factor (F-factor)¹ of -30 dBm which is a nominal 12-dB improvement over the previous design. The maximum output power level of the device (~58 dBm) has been improved by about 18 dB with 12 dB being associated with the use of tunnel junction arrays in the mixers and 6 dB the result of the reduction of parasitic capacitances in the output circuit.

In wideband measurements, input waveforms consisting of a flat-weighted upchirp and a complementary downchirp were applied to the signal and reference ports of the convolver. The waveforms were generated by two superconductive tapped-delay-line filters⁷. The waveforms had chirp slopes of about 62 MHz/ns and were effectively truncated to instantaneous bandwidths of about 0.85 GHz by the 14-ns-long interaction length of the convolver. The resultant output waveform shown in Fig. 6(b) has a bandwidth of about 1.7 GHz. Use of flat-weighted chirps should yield a $(\sin x)/x$ response with a null-to-null width of 1.2 ns and peak relative side lobes of -13 dB. A null-to-null width of 1.5 ns was observed with excessively high -7 dB side-lobe levels. These distortions are attributed primarily to mixer products produced from undesired leakage of input signal onto the output line and inadequate balance in the taps.

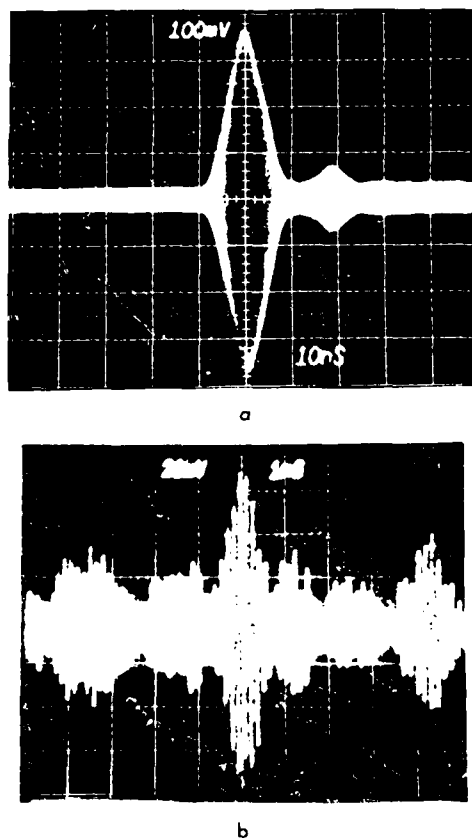


Fig. 6 Output waveform of junction ring convolver with inputs (a) of two 14-ns-duration gated CW input tones and (b) of two linearly chirped waveforms.

Extending Time-Bandwidth Product

The maximum potential signal-processing gain of an analog device is equal to its time-bandwidth (TB) product, where T , the interaction time, is the total delay length of the device over which the waveform is adequately sampled and B , the bandwidth, is limited to the frequency range over which the amplitude and phase response of the device is well behaved. Adequate sampling requires that the time delay between any two complex samples of the waveform not exceed $1/B$. The convolver design described in this report has a maximum tap-delay spacing of about 0.47 ns, for a potential signal processing bandwidth slightly greater than 2 GHz, and a delay time of about 14 ns; thus it has a nominal TB product of 28. Progress has been made in both the technology required to realize longer interaction lengths⁸ and in conceptual designs which incorporate substantially larger numbers of composite tap/mixer sections.

A "daisy-wheel" delay line structure, shown in Fig. 7, has been conceived and investigated as an alternative to the present "meander-line" structure. The modified structure will maximize the utilization of surface area on the round substrates. To have a TB product of 100, a like number of mixers is required. The mixers and output lines will be located around the outer edges of the "daisy-wheel" design. A new tap design with a symmetrical structure and very short transmission lines leads will improve "mixer balance" for improved spurious suppression. Design studies indicate that a convolver with a TB product of 100 can be fabricated on 125- μ m-thick, 7.6-cm-diameter substrates. Silicon and sapphire substrates with these dimensions are commercially available. Thinner substrates under development at Lincoln Laboratory would allow much greater circuit density and correspondingly larger convolver TB products.

Discussion

Significant improvements have been realized in the development of a superconductive convolver for wideband analog signal processing. A new convolver design has been designed, fabricated and characterized with CW bursts and wideband waveforms. The new design is providing an 18-dB improvement in output power level. Present spurious signal levels are unacceptably high and design improvements have been proposed. Current technology would support the development of a superconductive convolver on a single dielectric substrate with a bandwidth of 2-5 GHz and a TB product of 100.

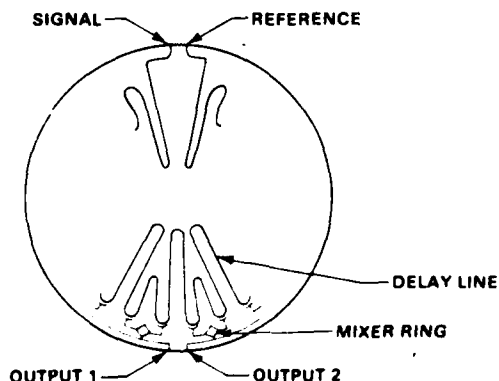


Fig. 7 Proposed "daisy-wheel" convolver structure.

Acknowledgements

The author gratefully acknowledges R. W. Ralston and J. H. Cafarella for their advice and guidance, E. M. Macedo for his reactive ion etching and tunnel junction work, R. S. Withers and A. C. Anderson for the superconductive tapped delay lines, J. H. Holtham for computer programming, A. P. Denneno and G. L. Fitch for photomask generation, C. M. Vanaria and P. R. Phinney for photolithography, J. Hamer for niobium films, and S. S. Cupoli for measurements.

REFERENCES

1. S. A. Reible, A. C. Anderson, P. V. Wright, R. S. Withers and R. W. Ralston, "Superconductive Convolver," IEEE Trans. Magn., vol. MAG-19, no. 3, pp. 475-480 (1983)
2. S. A. Reible, "Wideband Analog Signal Processing with Superconductive Circuits," 1982 Ultrasonics Symp. Proc. New York: IEEE, 1982, pp. 190-201.
3. J. H. Cafarella, J. A. Alusow, W. M. Brown and E. Stern, "Programmable Matched Filtering with Acoustoelectric Convolver in Spread-Spectrum Systems," 1975 Ultrasonics Symp. Proc. New York: IEEE, 1975, pp. 205-208.
4. S. A. Reible, "Acoustoelectric Convolver Technology for Spread Spectrum Communications," IEEE Trans. Microwave Theory and Tech., vol. MTT-29, no. 5, pp. 463-473 (1981).
5. S. A. Reible, "Reactive Ion Etching in the Fabrication of Niobium Tunnel Junctions," IEEE Trans. Magn., vol. MAG-17, no. 1, pp. 303-306 (1979).
6. E. L. Adler, "Electromagnetic Long-Line Effects in SAW Convolver," 1980 Ultrasonics Symp. Proc. New York: IEEE, 1980, pp. 82-87.
7. R. S. Withers, A. C. Anderson, P. V. Wright, and S. A. Reible, "Superconductive Tapped Delay Lines for Microwave Analog Signal Processing," IEEE Trans. Magn., vol. MAG-19, no. 3, pp. 480-484 (1983).
8. R. S. Withers, A. C. Anderson, J. B. Green and S. A. Reible, "Superconductive Delay-Line Technology and Applications," to be presented at the 1984 Applied Superconductivity Conference, San Diego, CA.

UNCLASSIFIED

SECURITY CLASSIFICATION OF THIS PAGE (When Data Entered)

REPORT DOCUMENTATION PAGE		READ INSTRUCTIONS BEFORE COMPLETING FORM
1. REPORT NUMBER ESD-TR-84-293	2. GOVT ACCESSION NO. AD-A152 703	3. RECIPIENT'S CATALOG NUMBER
4. TITLE (and Subtitle) Research on Superconductive Signal-Processing Devices		5. TYPE OF REPORT & PERIOD COVERED Annual Report 1 October 1983 — 30 September 1984
		6. PERFORMING ORG. REPORT NUMBER None
7. AUTHOR(s) R.W. Ralston		8. CONTRACT OR GRANT NUMBER(s) F19628-85-C-0002
9. PERFORMING ORGANIZATION NAME AND ADDRESS Massachusetts Institute of Technology Lincoln Laboratory, P.O. Box 73 Lexington, MA 02173-0073		10. PROGRAM ELEMENT, PROJECT, TASK AREA & WORK UNIT NUMBERS Program Element No.61102F Project No.2300
11. CONTROLLING OFFICE NAME AND ADDRESS Air Force Office of Scientific Research Bolling AFB, DC 20332		12. REPORT DATE 30 November 1984
		13. NUMBER OF PAGES 78
14. MONITORING AGENCY NAME & ADDRESS (if different from Controlling Office) Electronic Systems Division Hanscom AFB, MA 01731		15. SECURITY CLASS. (of this Report) Unclassified
		15a. DECLASSIFICATION DOWNGRADING SCHEDULE
16. DISTRIBUTION STATEMENT (of this Report) Approved for public release; distribution unlimited.		
17. DISTRIBUTION STATEMENT (of the abstract entered in Block 20, if different from Report)		
18. SUPPLEMENTARY NOTES None		
19. KEY WORDS (Continue on reverse side if necessary and identify by block number) convolver convolution time integrating correlator superconductive signal processing ring correlator		
20. ABSTRACT (Continue on reverse side if necessary and identify by block number) A new technology utilizing superconductive components to realize convolvers and correlators that are capable of processing analog signals having bandwidths from 2-20 GHz is being developed. The technology has two key features: (1) low-loss and low-dispersion electromagnetic striplines provide tapped delay on compact substrates; and (2) superconductive tunnel junctions provide efficient low-noise mixing and high-speed sampling circuits. A convolver with a time-bandwidth product of 28 has been demonstrated. Projections indicate that superconductive technology should support analog devices with time-bandwidth products of 1000 or greater.		
ORIGINATOR - SUPPLIED KEY WORD INCLUDE:		

END

FILMED

5--85

DTIC